Table 3. Classification of Highly (>3-Fold) Expressed Genes in ASC According to Gene Ontology Terms

Category	% of genes in category	% of genes in list in category	P value
0007067: Mitosis	1.3	11.4	4.43×10^{-24}
0000279: M phase	1.8	12.4	6.87×10^{-22}
0000278: Mitotic cell cycle	2.2	12.7	2.53×10^{-19}
0007049: Cell cycle	7.0	21.1	3.23×10^{-16}
0007059: Chromosome segregation	0.31	4.14	6.51×10^{-12}
0006260: DNA replication	1.3	7.32	9.94×10^{-12}
0007088: Regulation of mitosis	0.34	3.82	3.10×10^{-10}
0000070: Mitotic sister chromatid segregation	0.15	2.86	3.11×10^{-10}
0051301: Cell division	0.79	5.41	3.30×10^{-10}
0006955: Immune response	5.7	14.9	1.15×10^{-9}
0007017: Microtubule-based process	1.6	7.32	1.60×10^{-9}
0007093: Mitotic checkpoint	0.13	2.54	2.01×10^{-9}
0000074: Regulation of progression through cell cycle	4.5	12.7	2.77×10^{-9}
0006259: DNA metabolism	4.8	13.1	5.12×10^{-9}
0006952: Defense response	6.2	15.2	7.53×10^{-9}
0009613: Response to pest, pathogen or parasite	3.5	10.8	8.31×10^{-9}
0000075: Cell cycle checkpoint	0.44	3.82	9.71×10^{-9}
0009607: Response to biotic stimulus	6.6	15.6	1.32×10^{-8}
0043207: Response to external biotic stimulus	3.7	10.8	1.73×10^{-8}
0006950: Response to stress	9.2	19.1	3.41×10^{-8}
0031577: Spindle checkpoint	0.084	1.91	7.56×10^{-8}
0007018: Microtubule-based movement	0.87	4.77	8.72×10^{-8}
0006954: Inflammatory response	1.6	6.05	9.52×10^{-7}
0009605: Response to external stimulus	5.9	12.7	4.21×10^{-6}
0050896: Response to stimulus	16	25.8	4.24×10^{-6}
0031649: Heat generation	0.046	1.27	4.68×10^{-6}
0007052: Mitotic spindle organization and biogenesis	0.153	1.91	5.28×10^{-6}
0000226: Microtubule cytoskeleton organization and biogenesis	0.649	3.51	5.55×10^{-6}
0007010: Cytoskeleton organization and biogenesis	4.39	10.1	8.14×10^{-6}
0000067: DNA replication and chromosome cycle	0.0993	1.59	8.43×10^{-6}
0007051: Spindle organization and biogenesis	0.168	1.91	9.76×10^{-6}

ASC, adipose tissue-derived mesenchymal stem cells.

ing VEGF, HGF and SDF-1α.[4,5,10] To compare the proteins secreted by cultured ASC and BM-MSC, we used ELISA to investigate the production of several angiogenic and growth factors from ASC and BM-MSC cultures (**Figure 4**). As compared with BM-MSC, ASC secreted significantly larger amounts of not only HGF and VEGF, which are growth and angiogenic factors, but also PAI-1 and IL-6, which are adipokines. On the other hand, BM-MSC secreted significantly larger amounts of SDF-1α, which is a cell migration-related chemokine, than ASC. There was no significant difference between ASC and BM-MSC for several secreted adipokines, such as adiponectin and TNF-α.

Discussion

In this study, we examined the differences between ASC and BM-MSC in proliferation, differentiation, gene expression and secreted proteins. We showed that (1) ASC are more proliferative than BM-MSC, although there is no difference in differentiation into adipocytes or osteocytes; (2) genes associated with mitosis, inflammation and stress response are highly expressed in ASC; (3) genes associated with regulation of organ development, morphogenesis and cell migration are highly expressed in BM-MSC; and (4) ASC secrete significantly larger amounts of growth factors and inflammatory cytokines than BM-MSC, although BM-MSC secrete significantly larger amounts of chemokine than ASC.

In terms of differentiation, both ASC and BM-MSC differentiated into adipocytes and osteocytes, and there was no difference between them in adipogenesis in our quantitative analysis. A previous report demonstrated that BM-MSC had distinct osteogenic differentiation capability in comparison with ASC,[18] although we did not evaluate difference in osteogenesis between ASC and BM-MSC. Indeed, osteomodulin, which is an osteogenesis-related gene, was upregulated in BM-MSC in comparison with ASC (**Table 2**). Therefore, BM-MSC might have more osteogenic potential than ASC. These findings suggest that ASC and BM-MSC have multilineage potential and an equivalent potential to differentiate into unfavorable cells. Under these conditions, we found that ASC proliferated more rapidly than BM-MSC, and expanded 4-fold as much BM-MSC in approximately 2 weeks. Lee et al compared the proliferation and gene expression profile of human ASC and BM-MSC,[19] and also demonstrated that ASC differ from BM-MSC in terms of proliferation according to culture medium. A large number of MSC are needed for cell transplantation, so rapid proliferation of ASC ex vivo is thought to be a favorable source of transplanted cells in the acute clinical setting, although there remain prob-

Table 4. Classification of Highly (>3-Fold) Expressed Genes in BM-MSC According to Gene Ontology Terms

Category	% of genes in category	% of genes in list in category	P value
0048513: Organ development	8.86	21.9	5.02×10^{-12}
0008283: Cell proliferation	5.07	15.4	1.77×10^{-11}
0040007: Growth	2.18	9.62	4.23×10^{-11}
0009653: Morphogenesis	8.46	20.6	5.90×10^{-11}
0007275: Development	21.1	37.1	1.64×10^{-10}
0016049: Cell growth	1.53	7.56	6.82×10^{-10}
0016477: Cell migration	1.88	8.24	1.29×10^{-9}
0001558: Regulation of cell growth	1.31	6.52	8.83×10^{-9}
0007155: Cell adhesion	5.82	14.7	1.47×10^{-8}
0001501: Skeletal development	1.73	7.21	3.42×10^{-8}
0000902: Cellular morphogenesis	4.19	11.3	1.92×10^{-7}
0040008: Regulation of growth	1.64	6.52	3.21×10^{-7}
0009887: Organ morphogenesis	3.96	10.6	5.31×10^{-7}
0050678: Regulation of epithelial cell proliferation	0.0687	1.71	6.13×10^{-7}
0051674: Localization of cell	2.87	8.59	1.10×10^{-6}
0007626: Locomotory behavior	3.16	8.93	1.92×10^{-6}
0050673: Epithelial cell proliferation	0.084	1.71	2.17×10^{-6}
0006952: Defense response	6.27	13.7	2.26×10^{-6}
0009607: Response to biotic stimulus	6.59	14.1	3.12×10^{-6}
0045785: Positive regulation of cell adhesion	0.045	1.37	3.46×10^{-6}
0042127: Regulation of cell proliferation	3.32	8.93	4.56×10^{-6}
0050874: Organismal physiological process	16.7	27.1	4.75×10^{-6}

BM-MSC, bone marrow-derived mesenchymal stem cells.

lems concerning tumorigenesis and instability.

In this study, we carried out a comprehensive analysis in rat ASC and BM-MSC using microarrays. Interestingly, there was a considerable difference between the gene profile of our data and that of Lee et al,[19] who demonstrated that highly expressed genes in ASC accounted for less than 1% of all genes, and keratin 18, thrombospondin 1 and heat shock protein were included in the list of genes upregulated in ASC as compared with BM-MSC. Their human study was of 16–84-year-old patients undergoing arthroplasty and abdominoplasty, whereas we used 6-week-old rats. It is possible that differences in species and culture conditions, as well as age, contributed to these differences in gene expression.

We demonstrated that many of the genes that were highly expressed in ASC could be classified into categories such as mitosis, cell cycle and inflammatory cytokines, suggesting that ASC are more proliferative than BM-MSC. Thus, ASC transplant may not be superior to BM-MSC in terms of improvement of cardiac function in acute myocardial infarction, although it might be expected that ASC would contribute more to cell proliferation because of their secretion of VEGF and HGF. Also, ASC might initiate a stronger inflammatory response, because of the significantly increased upregulation of genes associated with inflammation as compared with BM-MSC. On the other hand, many of the genes that were highly expressed in BM-MSC were classified into categories such as organ development and morphogenesis. BM-MSC upregulated the expression of genes associated with cardiogenesis and angiogenesis, such as Wisp2, jagged1 and insulin-like growth factor binding protein 4 (IGFBP4). In particular, jagged1 and IGFBP4 have been reported to induce cardiogenesis and angiogenesis, respectively, via activation of notch signals and inhibition of Wnt signals.[20,21] Indeed, a previous report demonstrated that BM-MSC transplantation into the infarcted heart induces cardiogenesis and angiogenesis.[22–24] On the other hand, ASC are also reported to be able to differentiate into cardiomyocytes.[25] Therefore, ASC and BM-MSC both might improve cardiac function by supplementing cardiomyocytes, as well as in a paracrine manner, although we did not investigate differences in differentiation into cardiomyocytes between them.

BM-derived mononuclear cells and MSC have been used for therapeutic angiogenesis in ischemic disease.[26,27] MSC are thought to be more effective than mononuclear cells as a source of transplanted cells because MSC secrete larger amounts of growth factors.[26] Recent studies suggest that MSC exert tissue regeneration not only by differentiation into specific cell types, but also through paracrine actions, secreting various kinds of angiogenic and cytoprotective factors,[5,10] as shown in the present study. A recent report has shown that the combination of VEGF and MSC can enhance angiogenesis after acute myocardial infarction in rats.[28] Additionally, a previous study demonstrated that BM-MSC activate cardiac progenitor cells, which have the ability to differentiate into cardiomyocytes, in a paracrine manner in vitro and in vivo.[29,30] HGF and SDF-1α improve cardiac function via the activation of cardiac progenitor cells.[31] In our study, both ASC and BM-MSC secreted various cytokines and chemokines that are related to angiogenesis and cardiogenesis.

Although ASC are used as an adequate transplanted cell type for the treatment of ischemic limb disease,[32] ASC secrete larger amounts of not only inflammatory cytokines, such as IL-6, but also PAI-1 which promotes coagulation. In our gene analysis, several genes associated with other inflammatory cytokines and chemokines were upregulated in ASC. Not only the gene analysis but also the ELISA results suggested that ASC evoke more inflammation and thrombogenesis than BM-MSC. Therefore, ASC transplantation might be a more useful

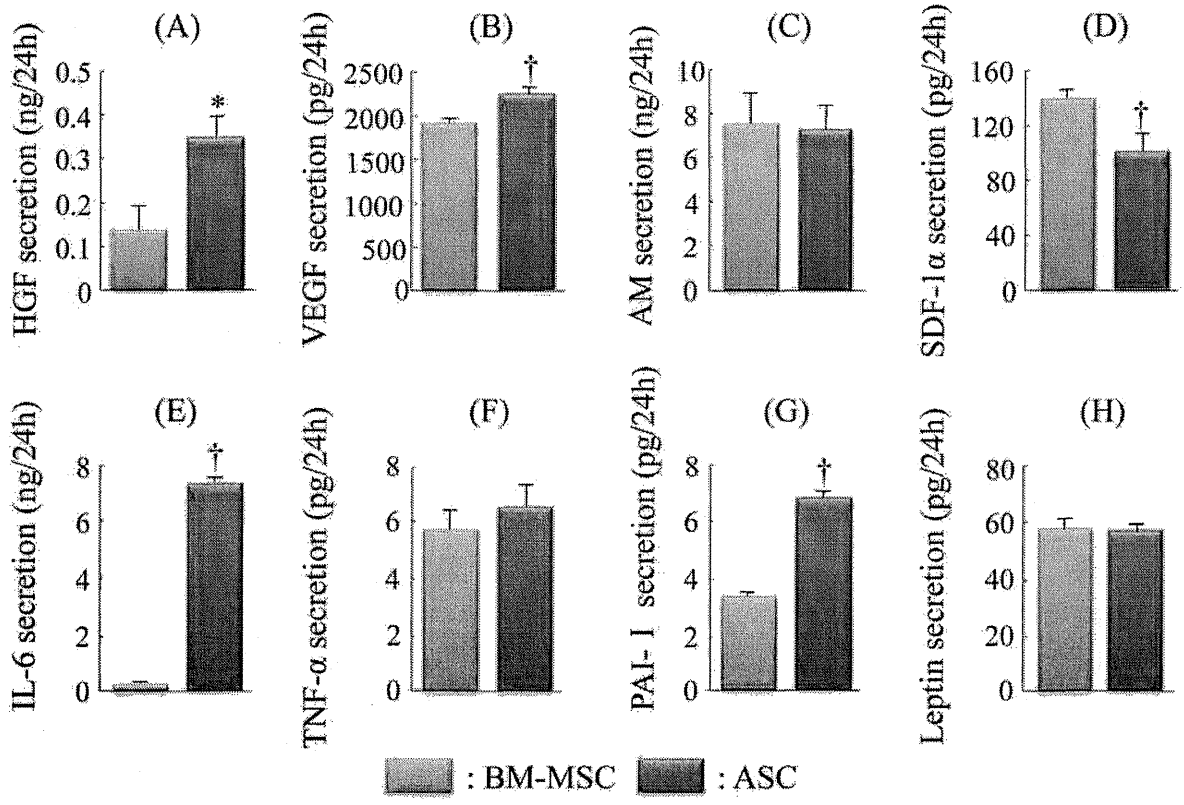

Figure 4. Secretory proteins from adipose tissue-derived mesenchymal stem cells (ASC: red) and bone marrow-derived mesenchymal stem cells (BM-MSC: blue). Conditioned media from ASC and BM-MSC were collected after incubation for 24h in complete medium. Hepatocyte growth factor (HGF, **A**), vascular endothelial growth factor (VEGF, **B**), adrenomedullin (AM, **C**), stem cell-derived factor-1α (SDF-1α, **D**), interleukin-6 (IL-6, **E**), tumor necrosis factor-α (TNF-α, **F**), plasminogen activator inhibitor-1 (PAI-1, **G**), and leptin (**H**) in conditioned media were measured by enzyme-linked immunosorbent assay. Values are mean±standard error of the mean. *P<0.05, †P<0.01 vs. BM-MSC.

treatment for chronic ischemia without severe inflammation.

In this study, we investigated ASC and BM-MSC obtained from young, 6-week-old rats, and we did not examine differences among various generations of rats. A previous report showed that MSC are subject to molecular genetic changes, such as alterations in p53, HGF and VEGF, during aging.[33] Our results might reflect the character of MSC obtained from young rats, contributing to difference from results in humans.[18] We need to further investigate differences between ASC and BM-MSC not only derived from rats but also derived from humans of various ages.

Conclusion

We have demonstrated difference in proliferation and gene expression between ASC and B-MSC, and accordingly, we suggest the importance of selecting the appropriate cell type for transplantation according to the therapeutic indication.

Acknowledgments

This work was supported by research grants for Human Genome Tissue Engineering 009 from the Ministry of Health, Labor and Welfare, and the Industrial Technology Research Grant Program from the New Energy and Industrial Technology Development Organization (NEDO) of Japan.

References

1. Pittenger MF, Mackay AM, Beck SC, Jaiswal RK, Douglas R, Mosca JD, et al. Multilineage potential of adult human mesenchymal stem cells. *Science* 1999; **284:** 143–147.
2. Minguell JJ, Erices A, Conget P. Mesenchymal stem cells. *Exp Biol Med* 2001; **226:** 507–520.
3. Prockop DJ. Marrow stromal cells as stem cells for nonhematopoietic tissues. *Science* 1997; **276:** 71–74.
4. Nagaya N, Fujii T, Iwase T, Ohgushi H, Itoh T, Uematsu M, et al. Intravenous administration of mesenchymal stem cells improves cardiac function in rats with acute myocardial infarction through angiogenesis and myogenesis. *Am J Physiol* 2004; **287:** 2670–2676.
5. Nagaya N, Kangawa K, Itoh T, Iwase T, Murakami S, Miyahara Y, et al. Transplantation of mesenchymal stem cells improves cardiac function in a rat model of dilated cardiomyopathy. *Circulation* 2005; **112:** 1128–1135.
6. Kinnaird T, Stabile E, Burnett MS, Shou M, Lee CW, Barr S, et al. Local delivery of marrow-derived stromal cells augments collateral perfusion through paracrine mechanisms. *Circulation* 2004; **109:** 1543–1549.
7. Chen S, Liu Z, Tian N, Zhang J, Yei F, Duan B, et al. Intracoronary transplantation of autologous bone marrow mesenchymal stem cells for ischemic cardiomyopathy due to isolated chronic occluded left anterior descending artery. *J Invasive Cardiol* 2006; **18:** 552–556.
8. Chen SL, Fang WW, Ye F, Liu YH, Qian J, Shan SJ, et al. Effect on left ventricular function of intracoronary transplantation of autologous bone marrow mesenchymal stem cell in patients with acute myocardial infarction. *Am J Cardiol* 2004; **94:** 92–95.
9. De Ugarte DA, Morizono K, Elbarbary A, Alfonso Z, Zuk PA, Zhu

M, et al. Comparison of multi-lineage cells from human adipose tissue and bone marrow. *Cells Tissues Organs* 2003; **174:** 101–109.
10. Kinnaird T, Stabile E, Burnett MS, Lee CW, Barr S, Fuchs S, et al. Marrow-derived stromal cells express genes encoding a broad spectrum of arteriogenic cytokines and promote in vitro and in vivo arteriogenesis through paracrine mechanisms. *Circ Res* 2004; **94:** 678–685.
11. Zuk PA, Zhu M, Mizuno H, Huang J, Futrell JW, Katz AJ, et al. Multilineage cells from human adipose tissue: Implications for cell-based therapies. *Tissue Eng* 2001; **7:** 211–228.
12. Miyahara Y, Nagaya N, Kataoka M, Yanagawa B, Tanaka K, Hao H, et al. Monolayered mesenchymal stem cells repair scarred myocardium after myocardial infarction. *Nature Med* 2006; **12:** 459–465.
13. Moon MH, Kim SY, Kim YJ, Kim SJ, Lee JB, Bae YC, et al. Human adipose tissue-derived mesenchymal stem cells improve postnatal neovascularization in a mouse model of hindlimb ischemia. *Cell Physiol Biochem* 2006; **17:** 279–290.
14. Gronthos S, Franklin DM, Leddy HA, Robey PG, Storms RW, Gimble JM. Surface protein characterization of human adipose tissue-derived stromal cells. *J Cell Physiol* 2001; **189:** 54–63.
15. Wakitani S, Saito T, Caplan AI. Myogenic cells derived from rat bone marrow mesenchymal stem cells exposed to 5-azacytidine. *Muscle Nerve* 1995; **18:** 1417–1426.
16. Solchaga LA, Penick K, Porter JD, Goldberg VM, Caplan AI, Welter JF. FGF-2 enhances the mitotic and chondrogenic potentials of human adult bone marrow-derived mesenchymal stem cells. *J Cell Physiol* 2005; **203:** 398–409.
17. Ohnishi S, Yasuda T, Kitamura S, Nagaya N. Effect of hypoxia on gene expression of bone marrow-derived mesenchymal stem cells and mononuclear cells. *Stem Cells* 2007; **25:** 1166–1177.
18. Hayashi O, Katsube Y, Hirose M, Ohgushi H, Ito H. Comparison of osteogenic ability of rat mesenchymal stem cells from bone marrow, periosteum, and adipose tissue. *Calcif Tissue Int* 2008; **82:** 238–247.
19. Lee RH, Kim B, Choi I, Kim H, Choi HS, Suh K, et al. Characterization and expression analysis of mesenchymal stem cells from human bone marrow and adipose tissue. *Cell Physiol Biochem* 2004; **14:** 311–324.
20. Zhu W, Shiojima I, Ito Y, Li Z, Ikeda H, Yoshida M, et al. IGFBP-4 is an inhibitor of canonical Wnt signalling required for cardiogenesis. *Nature* 2008; **454:** 345–349.
21. Boni A, Urbanek K, Nascimbene A, Hosoda T, Zheng H, Delucchi F, et al. Notch1 regulates the fate of cardiac progenitor cells. *Proc Natl Acad Sci USA* 2008; **105:** 15529–15534.
22. Tang XL, Rokosh DG, Guo Y, Bolli R. Cardiac progenitor cells and bone marrow-derived very small embryonic-like stem cells for cardiac repair after myocardial infarction. *Circ J* 2010; **74:** 390–404.
23. Hosoda T, Kajstura J, Leri A, Anversa P. Mechanisms of myocardial regeneration. *Circ J* 2010; **74:** 13–17.
24. Tsubokawa T, Yagi K, Nakanishi C, Zuka M, Nohara A, Ino H, et al. Impact of anti-apoptotic and -oxidative effects of bone marrow mesenchymal stem cells with transient overexpression of heme oxygenase-1 on myocardial ischemia. *Am J Physiol* 2010; **298:** 1320–1329.
25. Choi YS, Dusting GJ, Stubbs S, Arunothayaraj S, Han XL, Collas P, et al. Differentiation of human adipose-derived stem cells into beating cardiomyocytes. *J Cell Mol Med* 2010; **14:** 878–889.
26. Iwase T, Nagaya N, Fujii T, Itoh T, Murakami S, Matsumoto T, et al. Comparison of angiogenic potency between mesenchymal stem cells and mononuclear cells in a rat model of hindlimb ischemia. *Cardiovasc Res* 2005; **66:** 543–551.
27. Kinnaird T, Stabile E, Burnett MS, Epstein SE. Bone-marrow-derived cells for enhancing collateral development: Mechanisms, animal data, and initial clinical experiences. *Circ Res* 2004; **95:** 354–363.
28. Tang J, Wang J, Zheng F, Kong X, Guo L, Yang J, et al. Combination of chemokine and angiogenic factor genes and mesenchymal stem cells could enhance angiogenesis and improve cardiac function after acute myocardial infarction in rats. *Mol Cell Biochem* 2010; **339:** 107–118.
29. Nakanishi C, Yamagishi M, Yamahara K, Hagino I, Mori H, Sawa Y, et al. Activation of cardiac progenitor cells through paracrine effects of mesenchymal stem cells. *Biochem Biophys Res Commun* 2008; **374:** 11–16.
30. Hatzistergos KE, Quevedo H, Oskouei BN, Hu Q, Feigenbaum GS, Margitich IS, et al. Bone marrow mesenchymal stem cells stimulate cardiac stem cell proliferation and differentiation. *Circ Res* 2010; **107:** 913–922.
31. Rota M, Padin-Iruegas ME, Misao Y, De Angelis A, Maestroni S, Ferreira-Martins J, et al. Local activation or implantation of cardiac progenitor cells rescues scarred infarcted myocardium improving cardiac function. *Circ Res* 2008; **103:** 107–116.
32. Bhang SH, Cho SW, Lim JM, Kang JM, Lee TJ, Yang HS, et al. Locally delivered growth factor enhances the angiogenic efficacy of adipose-derived stromal cells transplanted to ischemic limbs. *Stem Cells* 2009; **27:** 1976–1986.
33. Wilson A, Shehadeh LA, Yu H, Webster KA. Age-related molecular genetic changes of murine bone marrow mesenchymal stem cells. *BMC Genomics* 2010; **229:** 7–11.

Journal of Molecular and Cellular Cardiology 53 (2012) 420–428

Contents lists available at SciVerse ScienceDirect

Journal of Molecular and Cellular Cardiology

journal homepage: www.elsevier.com/locate/yjmcc

Original article

Systemic transplantation of allogenic fetal membrane-derived mesenchymal stem cells suppresses Th1 and Th17 T cell responses in experimental autoimmune myocarditis

Makiko Ohshima [a], Kenichi Yamahara [a,*], Shin Ishikane [a], Kazuhiko Harada [c], Hidetoshi Tsuda [a], Kentaro Otani [a], Akihiko Taguchi [a,e], Mikiya Miyazato [e], Shinji Katsuragi [b], Jun Yoshimatsu [b], Makoto Kodama [f], Kenji Kangawa [d], Tomoaki Ikeda [a,b,g]

[a] Department of Regenerative Medicine and Tissue Engineering, National Cerebral and Cardiovascular Center, Osaka, Japan
[b] Department of Perinatology, National Cerebral and Cardiovascular Center, Osaka, Japan
[c] Department of Pharmacy, National Cerebral and Cardiovascular Center, Osaka, Japan
[d] Department of Biochemistry, National Cerebral and Cardiovascular Center, Osaka, Japan
[e] Department of Regenerative Medicine Research, Biomedical Research Innovation, Hyogo, Japan
[f] Division of Cardiology, Niigata University Graduate School of Medical and Dental Science, Niigata, Japan
[g] Department of Obstetrics and Gynecology, Mie University School of Medicine, Mie, Japan

ARTICLE INFO

Article history:
Received 7 February 2012
Received in revised form 7 June 2012
Accepted 28 June 2012
Available online 13 July 2012

Keywords:
Acute myocarditis
Mesenchymal stem cells
Fetal membrane
Allogenic transplantation
T cell response

ABSTRACT

We have reported that systemic administration of autologous bone marrow or allogenic fetal membrane (FM)-derived mesenchymal stem cells (MSCs) similarly attenuated myocardial injury in rats with experimental autoimmune myocarditis (EAM). Since rat EAM is a T-helper (Th) cell-mediated autoimmune disease, and recent evidence has indicated that both autologous and allogenic MSCs exert an immunosuppressive effect on Th cell activity, we focused on Th cell differentiation in allogenic FM-MSC administered EAM rats. EAM was induced in Lewis rats by injecting porcine cardiac myosin (day 0). Allogenic FM-MSCs, obtained from major histocompatibility complex mismatched ACI rats, were intravenously injected (5×10 cells/rat) on days 7, 10, or 14 (MSCd7, MSCd10, or MSCd14 groups, respectively). At day 21, echocardiography confirmed that reduced ejection fraction in the untreated EAM group ($63\pm2\%$) was significantly improved in the MSCd10 and MSCd14 groups (74 ± 1 and $75\pm2\%$, respectively, $P<0.01$). CD68 immunostaining revealed that prominent macrophage infiltration in the myocardium of the EAM group (1466 ± 93 cells/mm^2) was significantly decreased in the MSCd10 group (958 ± 139 cells/mm^2, $P<0.05$). To evaluate Th cell differentiation, we used flow cytometry to determine the percentage of interferon (IFN)-γ positive Th1 and interleukin (IL)-17 positive Th17 cells in peripheral CD4-positive Th cells. The percentage of Th1 cells at day 16 was significantly lower in the MSCd10 ($1.3\pm0.2\%$) and MSCd14 ($1.6\pm0.3\%$) groups compared to the EAM group ($2.4\pm0.3\%$, $P<0.05$), as was the percentage of Th17 cells in the MSCd10 group ($1.9\pm0.5\%$) compared to the EAM group ($2.2\pm0.9\%$, $P<0.05$). At day 21, infiltrating Th17 cells in myocardium were significantly decreased in the MSCd10 group (501 ± 132 cells/mm^2, $P<0.05$) compared to EAM (921 ± 109 cells/mm^2). In addition, human CD4+ Th cells co-cultured with human FM-MSCs exhibited reduced Th1 and Th17 cell-differentiation and proliferation, with increased expression of immunosuppressive molecules including indoleamine 2,3-dioxygenase 2 and IL-6 in co-cultured FM-MSCs. These results suggest that intravenous administration of allogenic FM-MSCs ameliorates EAM via the suppression of Th1/Th17 immunity.

1. Introduction

Experimental autoimmune myocarditis (EAM) induced by immunizing with cardiac myosin is a T cell-mediated autoimmune disease. We previously reported that CD8+ T cells are not required to induce myocarditis in rat EAM and that CD4+ helper T (Th) cells regulate its disease severity [1–3]. Activated Th cells secrete various cytokines which recruit and activate other inflammatory cells, such as macrophages, neutrophils, and mast cells [4]. Histological examination of hearts with EAM demonstrates the infiltration of inflammatory cells two weeks after immunization. An excess amount of cytokines and chemokines secreted from recruited inflammatory cells contributes to myocardial damage, and myocarditis peaks around the third week in EAM rats [5,6].

* Corresponding author at: Department of Regenerative Medicine and Tissue Engineering, National Cerebral and Cardiovascular Center, 5-7-1 Fujishirodai, Suita, Osaka 565-8565, Japan. Tel.: +81 6 6833 5012; fax: +81 6 6833 9865.
E-mail address: yamahara@ri.ncvc.go.jp (K. Yamahara).

0022-2828/$ – see front matter © 2012 Elsevier Ltd. All rights reserved.
doi:10.1016/j.yjmcc.2012.06.020

During the initiation of EAM, naïve CD4+ Th cells are traditionally thought to differentiate into interferon (IFN) γ-producing Th1 [7] and interleukin (IL)-4-producing Th2 cell subsets [8], and it has been assumed that the Th1/Th2 cytokine balance is important in the pathogenesis of EAM [8,9]. Recently, several reports have noted that IL-17-producing Th17 cells are involved in the development of EAM [10], because the severity of EAM is associated with the myocardial expression of IL-17 [11]. Therefore, in addition to the Th1/Th2 cytokine balance, the examination of Th17 cytokine is necessary to determine their pathological roles in EAM.

We have reported that intravenous injection of autologous bone-marrow (BM)-derived mesenchymal stem cells (BM-MSCs) and allogenic fetal membrane (FM)-derived MSC (FM-MSCs) ameliorates myocardial injury in rats with EAM [12,13]. Although we focused on the angiogenic effect and the paracrine action of transplanted MSCs on EAM in our previous study, we showed that allogenic FM-MSCs significantly reduced the proliferation and activity of T lymphocytes [12,13]. Accumulated evidence has indicated that MSCs modify CD4+ Th cell function [14]. MSC-induced inhibition of T cell proliferation leads to decreased IFN-γ production by Th1 cells and increased IL-4 production by Th2 cells, indicating a shift in T cells from an IFN-γ-dominant pro-inflammatory state to an IL-4-dominant anti-inflammatory state. In addition, recent reports indicate that MSC may inhibit Th17 differentiation [16]. Therefore, we speculated that administered MSCs in EAM rats would attenuate myocardial inflammation by altering Th1/Th2/Th17 immunity.

In this study, we investigated the mechanism by which allogenic FM-MSC administration ameliorates myocarditis in EAM rats, focusing on CD4+ Th cell function. We also examined the effect of allogenic FM-MSC on the differentiation of Th1/Th17 cells.

2. Materials and methods

2.1. Animals

Different strains of rats were used, based on their major histocompatibility complex (MHC) antigen disparities: Lewis rats (MHC haplotype: RT-1Al; Japan SLC, Hamamatsu, Japan) and August–Copenhagen–Irish (ACI) rats (MHC haplotype: RT-1Aa; Japan SLC). The experimental protocols were approved by the Animal Care Committee of the National Cerebral and Cardiovascular Center.

2.2. Preparation of rat and human FM-MSCs

To obtain rat FMs, pregnant ACI rats (15 days postconception) were sacrificed and their uteri were harvested and placed in PBS (Invitrogen, Carlsbad, CA) [12]. Human FMs were obtained following caesarean section of healthy donor mothers. Human amnion membranes (AMs) were separated from human FMs by mechanical peeling. All experiments using human FMs were approved by the Ethics Committee of the National Cerebral and Cardiovascular Center.

Rat FMs and human AMs were minced and digested with type II collagenase (300 U/ml; Worthington Biochemicals, Lakewood, NJ) for 1 h at 37 °C. After filtration through a mesh filter (100 μm; BD Biosciences, Bedford, MA) and centrifugation at 300×g for 5 min, the dissociated FM-derived cells were suspended in α-MEM supplemented with 10% FBS (Thermo Fisher Scientific Inc., Waltham, MA), 100 U/ml penicillin, and 100 μg/ml streptomycin (Invitrogen) and incubated at 37 °C in 5% CO_2. The population of adherent, spindle-shaped MSCs was expanded. In all experiments, FM-MSCs were used at passages 5–7.

2.3. Acute myocarditis model

Purified cardiac myosin was prepared from pig hearts according to the previously described procedure [17]. The antigen was dissolved at a concentration of 20 mg/ml in PBS containing 0.3 M KCl and mixed with an equal volume of complete Freund's adjuvant containing 6 mg/ml *Mycobacterium tuberculosis* (Difco Laboratories, Sparks, MD). Eight-week-old Lewis rats were injected with 0.1 ml of the antigen–adjuvant emulsion into each footpad and randomly divided into four groups: no transplantation, or FM-MSC administration on day 7, 10, or 14 after myosin injection (EAM, MSCd7, MSCd10, or MSCd14 groups, respectively). For FM-MSC transplantation, we intravenously injected 5×10^5 cells in 0.2 ml of PBS. Sham-operated rats and EAM rats (without FM-MSC administration) were injected with 0.2 ml of PBS on day 7.

2.4. Echocardiographic studies

Echocardiography was performed on day 21 after myosin injection [12]. Rats were anesthetized with isoflurane and a 12-MHz probe was used for M-mode imaging of two-dimensional echocardiography (Sonos 5500, Philips, Bothell, WA). The left ventricular systolic dimension (LVDs), left ventricular diastolic dimension (LVDd), anterior wall thickness (AWT), posterior wall thickness (PWT), fractional shortening (FS) and ejection fraction (EF) were measured. The echocardiography studies were performed with the investigators blinded to exposure and outcome.

2.5. Flow cytometric analysis of Th cell subsets

The presence of Th1, Th2, Th17, or regulatory T (Treg) cells was determined by measuring IFN-γ-, IL-4-, IL-17, or Foxp3-expressing CD4+ cells using flow cytometry [18]. Blood samples diluted 1:1 with RPMI 1640 medium (Invitrogen) were cultured with 60 ng/ml phorbol myristate acetate (PMA), 1.2 μg/ml ionomycin and 12 μg/ml brefeldin A (all from Sigma-Aldrich, St Louis, MO) for 4 h at 37 °C. After incubation with APC-conjugated anti-rat CD4 antibodies (BioLegend, San Diego, CA), cells were fixed and permeabilized, and further incubated with FITC-conjugated anti-rat IFN-γ (BioLegend), R-phycoerythrin (PE)-conjugated anti-rat IL-4 (BioLegend), PE-conjugated anti-rat IL-17A (BD Bioscience), or Alexa Fluor 488-conjugated anti-rat Foxp3 (eBioscience, San Diego, CA) antibody. Cells were then resuspended in 1% paraformaldehyde (PFA) and subjected to flow cytometric analysis (FACSCanto; BD Bioscience).

2.6. Immunohistochemical studies

For immunostaining of IL-17 and CD68, cardiac tissues were fixed with 4% PFA, embedded in paraffin blocks, and cut into 2 μm sections. For IFN-γ and IL-23 immunostaining, hearts were quickly frozen, cut into 5 μm sections, and fixed with 2% PFA for 30 s and acetone for 30 s [19]. After treatment with Protein Block (Dako Cytomation, Glostrup, Denmark), sections were incubated with rabbit anti-rat IL-17 (clone H-132; Santa Cruz Biotechnology, CA,), rabbit anti-rat IFN-γ (clone DB-1; BioLegend), mouse anti-rat CD68 (clone ED-1; Millipore, Bedford, MA), or rabbit anti-rat IL-23 (clone H-113; Santa Cruz) in diluent (DAKO Cytomation) overnight at 4 °C, followed by anti-mouse LSAB/HRP (Dako Cytomation) or anti-rabbit Envision+ system-HRP Labeled Polymer (Dako Cytomation) for 30 min. HRP-labeled sections were visualized with 0.5% diaminobenzidine (Dako Cytomation) and 0.03% H_2O_2, and counterstained with hematoxylin. For immunofluorescent staining, Alexa Fluor dye-conjugated anti-mouse or anti-rabbit IgG antibodies (1:1000, Invitrogen) were used as the secondary antibody and nuclei were stained with SYBR green I (1:10,000, Invitrogen). Sections were photographed using a digital microscope (BIOREVO BZ-9000; KEYENCE, Osaka, Japan), and the number of IL-17-, IFN-γ-, and CD68-positive cells was counted in 20 randomly selected fields per section using image processing software (WinROOF, Mitani Co. Ltd., Tokyo, Japan).

Table 1
Echocardiographic findings in all groups at day 21 after myosin injection.

		Sham	EAM	MSCd7	MSCd10	MSCd14
HR	(bpm)	427±12	370±15	378±7	386±14	378±16
AWT diastole	(mm)	1.5±0.0	2.1±0.1**	2.0±0.1**	1.8±0.0*†	1.9±0.1**
PWT diastole	(mm)	1.5±0.0	2.2±0.1**	2.1±0.1**	1.9±0.0**††§	2.0±0.0**
LVDs	(mm)	3.2±0.1	5.5±0.2**	5.3±0.2**	4.6±0.1**††§	4.5±0.2**††§
LVDd	(mm)	6.7±0.1	7.7±0.2**	7.9±0.2**	7.4±0.2	7.3±0.2

Sham: sham-operated rats given vehicle on day 7; EAM: myosin-treated rats given vehicle on day 7; MSCd7, MSCd10, MSCd14: myosin-treated rats given FM-MSCs (5×10^5 cells/animal) on days 7, 10, and 14 after myosin injection; HR: heart rate; AWT: anterior wall thickness; PWT: posterior wall thickness; LVDs: left ventricular systolic dimension; LVDd: left ventricular diastolic dimension. *P<0.05 and **P<0.01 vs. sham group, †P<0.05, ††P<0.01 vs. EAM group, §P<0.05 vs. MSCd7.

2.7. In vitro Th1/Th17 differentiation assay

Human peripheral blood CD4+ T cells (5×10^5 cells/well; Lonza, Walkersville, MD) were cultured with X-VIVO medium (Lonza) containing 2% FBS in anti-CD3- and anti-CD28-coated 24-well plates (clone OKT3 and CD28.2, respectively, BioLegend). To induce Th1 differentiation, medium was supplemented with recombinant IL-2 (10 ng/ml; HumanZyme, Chicago, IL), IL-12 (1 μg/ml; HumanZyme), and anti-human IL-4 antibody (1 μg/ml; clone 8D4-8; BioLegend) [15]. To induce Th17 differentiation, medium was supplemented with recombinant TGF-β, IL-1β, IL-6, and IL-23 (10 ng/ml; HumanZyme) [20]. During in vitro differentiation of CD4+ T cells, human BM-MSCs (Lonza) or FM-MSCs were co-cultured at 5×10^4 cells/well. After 5 days of co-culturing, T cells were separated from the MSC monolayer and counted with an automated cell counter (Countess, Invitrogen). T cells were stimulated with 60 ng/ml PMA, 1.2 μg/ml ionomycin, and 12 μg/ml brefeldin A (all from Sigma-Aldrich) for 4 h at 37 °C. Stimulated cells were labeled with APC-Cy7-conjugated anti-human CD4 antibodies (BioLegend), followed by fixation and permeabilization with BD FACS Lysing Solution and Permeabilizing Solution (BD Bioscience). Cells were then incubated with FITC- or PE-conjugated anti-human CD90 (BD Bioscience) and FITC-conjugated anti-human IFN-γ or PE-conjugated anti-human IL-17 (BioLegend) antibodies for a further 30 min, resuspended in 1% PFA, and subjected to flow cytometric analysis (FACSCanto, BD Bioscience).

2.8. Quantitative reverse-transcription polymerase chain reaction (qRT-PCR) analysis

Total RNA was extracted from isolated rat spleens or co-cultured human FM-MSCs using an RNeasy mini kit (Qiagen, Hilden, Germany). RNA was reverse-transcribed into cDNA using a Quantitect Reverse Transcription kit (Qiagen). PCR amplification was performed on a 7500 Real-Time PCR System (Applied Biosystems, Foster City, CA) using Power SYBR Green PCR Master Mix (Applied Biosystems). β-actin (for rat spleens) or human GAPDH (for FM-MSCs) was used as an internal control. Primer sequences are listed in Table 2.

2.9. Statistical analysis

All data are expressed as mean±SEM. Comparisons between two parameters were analyzed by using the unpaired Student's t-test. Comparisons of parameters among the groups were made by one-way analysis of variance (ANOVA) followed by Tukey's test. FACS data were analyzed by two-way repeated measures ANOVA. A value of P<0.05 was considered statistically significant.

3. Results

3.1. Improvement in cardiac function by allogenic administration of FM-MSCs

All rats with myocarditis survived during the observation period. Echocardiographic analysis on day 21 post myosin injection is summarized in Fig. 1 and Table 1. Allogenic FM-MSC transplantation improved FS and EF, as we reported previously (Fig. 1) [12]. Among the groups, the MSCd10 and MSCd14 (FM-MSC transplanted on days 10 and 14, respectively) groups showed significant improvement in FS (MSCd10: 38.5±1.0, MSCd14: 39.1±1.5, vs. EAM: 29.3±1.2%, P<0.01) and EF (MSCd10: 74.4±1.3, MSCd14: 74.9±2.2, vs. EAM: 62.6±2.1%, P<0.01). In addition, FM-MSC administration significantly decreased PWT at diastole (MSCd10: 1.9±0.0, vs. EAM: 2.2±0.1 mm, P<0.05) and LVDs (MSCd10: 4.6±0.1 vs. EAM: 5.5±0.2 mm, P<0.05), although AWT) at diastole and LVDd did not significantly differ between the groups (Table 1).

3.2. Reduced macrophage infiltration of myocardium after FM-MSC treatment

Immunohistochemical analysis of myocardial tissues on day 21 demonstrated that, compared to the untreated EAM group, the infiltration of CD68-positive macrophages was significantly attenuated in the MSCd10 group (958±139 cells/mm², n=11; P<0.05 vs. 1466±93 cells/mm², n=13) (Fig. 2). In the other cell transplanted groups, systemic injection of FM-MSC tended to suppress the myocardial infiltration of macrophages compared to the EAM group. (MSCd7: 1279±179 cells/mm², n=6; MSCd14: 1040±195 cells/mm², n=6).

3.3. Suppression of Th1/Th17 cells after FM-MSC treatment in EAM rats

In the FACS analysis, peripheral CD4+ Th cells were further subdivided based on the expression of IFN-γ (Th1) and IL-17 (Th17) [18] (Figs. 3 and 4). In FM-MSC-untreated EAM rats (the EAM group),

Table 2
Primer sequences used for qRT-PCR.

Gene	species	Forward	Reverse
IL-17	Rat	5′-TGTCCAAACGCCGAGGCCAA-3′	5′-AGGGCCTTCTGGAGCTCGCTT-3′
β-actin	Rat	5′-GCCCTAGACTTCGAGC-3′	5′-CTTTACGGATGTCAACGT-3′
IDO2	Human	5′-CCACAGACCGAATGTGAAGAC-3′	5′-TGTTGGCAATTTCCATCCAAGG-3′
HLA-G	Human	5′-CACGCACAGACTGACAGAATG-3′	5′-GCCATCGTAGGCATACTGTTCA-3′
IL-6	Human	5′-TTGGAAGGTTCAGGTTGTTTTCT-3′	5′-AATTCGGTACATCCTCGACGG-3′
GAPDH	Human	5′-GAGGCAGGGATGATGTTCTGGA-3′	5′-CAATGCCTCCTGCACCACCAA-3′

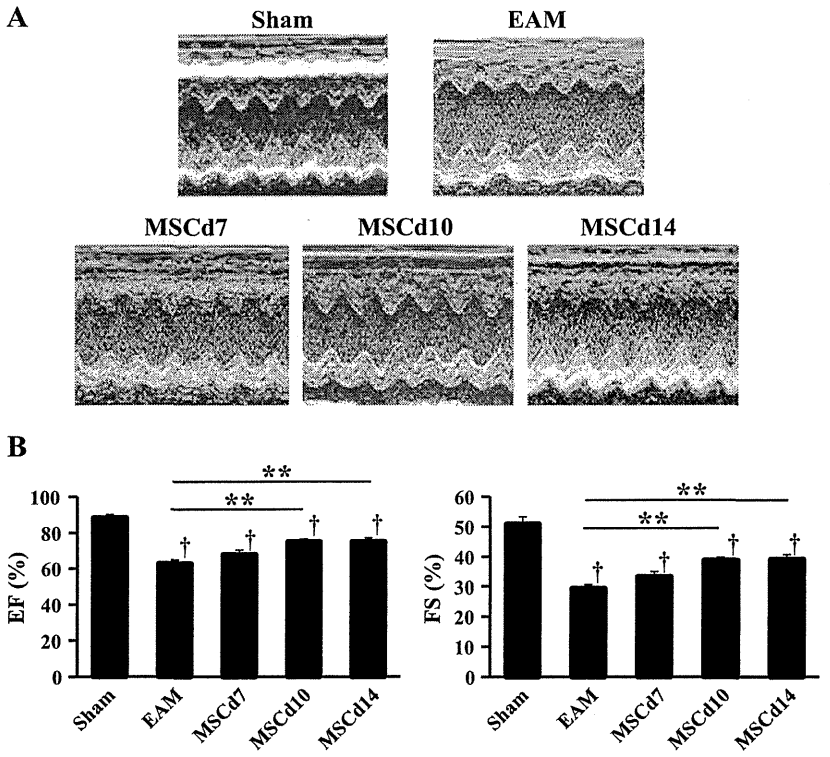

Fig. 1. Effects of allogenic FM-MSC transplantation on echocardiographic parameters in EAM. (A) Representative echocardiographic images showing poor movement in the EAM group compared to the sham group. Improved cardiac contractility was observed in the FM-MSC-administered groups at day 10 (MSCd10) and 14 (MSCd14) after the induction of myocarditis. (B, C) FM-MSC administration significantly improved EF and FS in the MSCd10 and MSCd14 groups. $^{**}P<0.01$ vs. EAM, †$P<0.05$ vs. MSCd7, n = 11–13.

there was an increase in Th1 cells until day 16 after myosin injection (2.4 ± 0.3% of CD4+ cells on day 16), which subsequently decreased gradually (1.1 ± 0.2% on day 36) (Fig. 3B). In the FM-MSC-treated groups, a decrease in the percentage of Th1 cells was observed. On day 16, the FM-MSC-treated MSCd10 and MSCd14 groups showed a significant decrease in the percentage of Th1 cells (MSCd10: 1.3 ± 0.2%, MSCd14: 1.6 ± 0.3% of CD4+ cells, $P<0.05$ vs. EAM), but no difference was seen between the EAM and MSCd7 groups.

As shown in Fig. 4B, the percentage of Th17 cells was substantially increased in the EAM group until day 16 (2.2 ± 0.9% of CD4+ cells on day 16) and decreased thereafter (1.0 ± 0.1% on day 21). Similar to what was found for Th1 cells, a significant decrease in Th17 cells was found in the FM-MSC-treated MSCd10 group (1.9 ± 0.5% on day 16, $P<0.05$ vs. EAM). On day 16, IL-17 mRNA expression in the spleen was markedly decreased in the MSCd10 group compared with the untreated EAM group ($P<0.001$ vs. EAM, n = 7 in each group).

Although we also examined other Th subsets in the peripheral blood of myocarditis rats, no significant changes in the Th2 or Treg were observed between the groups (data not shown).

3.4. Decreased infiltration of IFN-γ- and IL-17-positive cells in the myocardium following FM-MSC treatment

Immunohistochemical staining of IL-17 in EAM hearts on day 21 demonstrated that FM-MSC administration significantly decreased the infiltration of IL-17-postive cells in the MSCd10 group compared to the EAM group (MSCd10: 501 ± 132 vs. EAM: 921 ± 109 cells/mm², $P<0.05$; n = 9 in each group). (Figs. 5C, D) A similar tendency toward decreased infiltration of IL-17-positive cells was found in the other FM-MSC-transplanted groups (MSCd7: 534 ± 96 cells/mm², n = 11; MSCd14: 508 ± 77 cells/mm², n = 6). IFN-γ staining also revealed that there was a tendency for suppressed infiltration of IFN-γ+ cells following FM-MSC administration (MSCd10: 85 ± 20 vs. EAM: 196 ± 75 cells/mm², $P=0.17$, n = 10 in each group) (Figs. 5A, B).

3.5. Inhibition of Th1/Th17 differentiation in CD4+ T cells when co-cultured with MSCs

The effect of human FM-MSCs on Th1/Th17 differentiation was analyzed using human peripheral blood CD4+ T cells. After 5 days of culturing of CD4+ T cells under Th1-polarizing conditions, the number of CD4+ cells markedly increased ($7.1 \pm 0.4 \times 10^4$ cells/ml) and a significant number of Th1 cells appeared (IFN-γ+ cells/CD4+ cells: 13.9 ± 1.2%) (Fig. 6A). When co-cultured with FM-MSCs or BM-MSCs, the number of CD4+ T cells and the differentiation into Th1 cells were significantly suppressed (CD4+ cells: $1.8 \pm 0.4 \times 10^5$ cells/ml in FM-MSC, $3.1 \pm 0.3 \times 10^5$ cells/ml in BM-MSCs; Th1 cells: 1.8 ± 0.2% in FM-MSCs, 10.1 ± 1.0% in BM-MSCs, $P<0.01$ vs. control) (Figs. 6C, D). Compared to BM-MSCs, FM-MSCs significantly suppressed Th1 differentiation ($P<0.01$ vs. BM-MSCs) (Fig. 6C).

When human CD4+ T cells were stimulated for 5 days under Th17-differentiating conditions, the number of CD4+ cells and IL-17-expressing Th17 cells also increased (CD4+ cells: $3.8 \pm 1.6 \times 10^5$ cells/ml, IL-17+ cells/CD4+ cells: 6.8 ± 0.4%) (Figs. 6A, B). The presence of FM-MSCs as well as BM-MSCs significantly suppressed the number of CD4+ cells (FM-MSCs: $0.9 \pm 0.6 \times 10^5$ cells/ml, BM-MSCs: $1.3 \pm 1.5 \times 10^5$ cells/ml, $P<0.01$ vs. control) (Fig. 6F) and differentiation into Th17 cells (FM-MSCs: 1.5 ± 0.1%, BM-MSCs: 2.3 ± 0.3%, $P<0.01$ vs. control) (Fig. 6E).

Under Th17-polarizing culture conditions with CD4+ T cells, we also quantified the gene expression of immunosuppressive molecules including indoleamine 2,3-dioxygenase (IDO) 2, IL-6, and HLA-G in co-cultured FM-MSCs. The expression of IDO2 and IL-6 was significantly increased in co-cultured FM-MSCs (IDO2: 27.7 ± 11.0 fold,

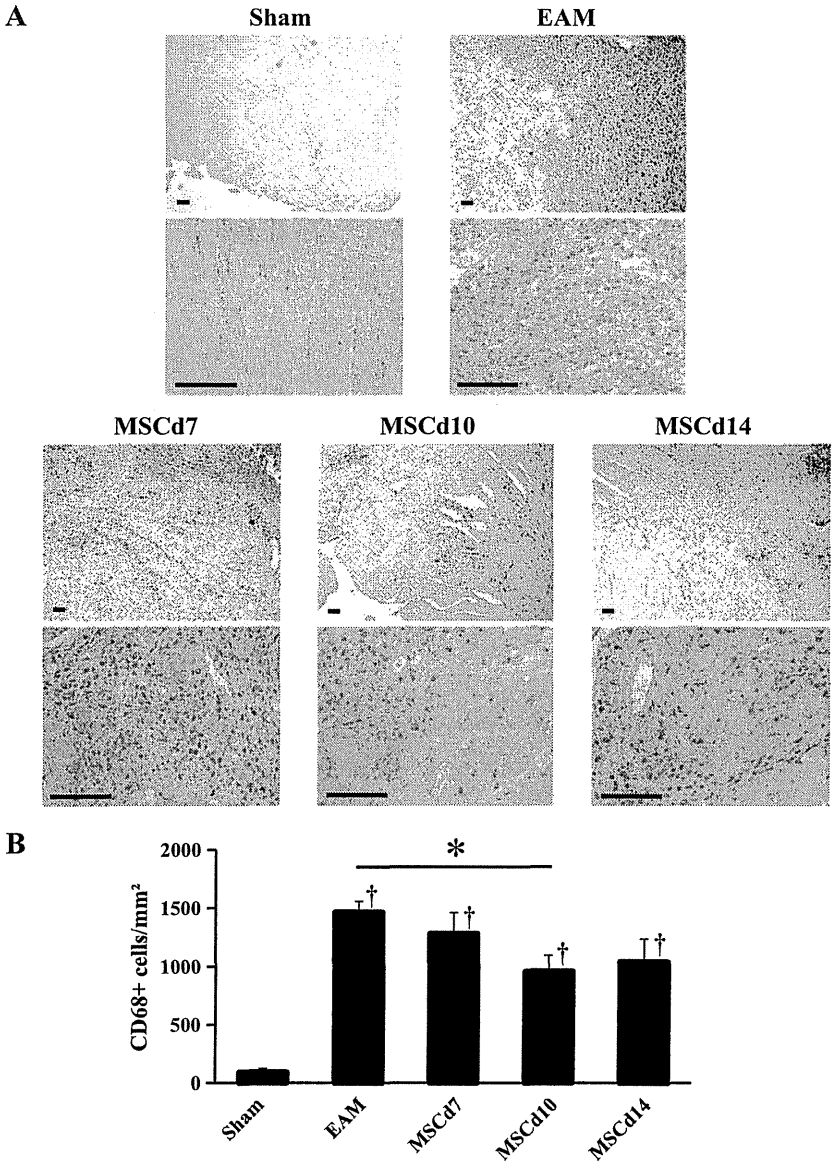

Fig. 2. Effects of allogenic FM-MSC administration on myocardial macrophage infiltration in EAM. (A) Representative myocardial sections of CD68 immunostaining demonstrate a decrease in CD68-positive cells after FM-MSC transplantation. (B) Quantitative counts of CD68-positive macrophages show a significant reduction in the MSCd10 group compared to the EAM group. Scale bars: 100 μm. *$P<0.05$ vs. EAM, †$P<0.05$ vs. sham. n=6-13.

IL-6: 23.7±8.9 fold, $P<0.05$ vs. control mono-cultured FM-MSCs). Co-cultured FM-MSCs also showed a tendency for increased gene expression of HLA-G (HLA-G: 3.8±1.5 fold, $P=0.096$ vs. control FM-MSCs).

4. Discussion

In this study, we elucidated the mechanisms involved in the therapeutic effects of FM-MSC transplantation in EAM, particularly focusing on the regulatory effect of FM-MSCs on Th cells. We demonstrated that 1) intravenous administration of allogenic FM-MSCs on the tenth day after myosin injection significantly improved both cardiac function and myocardial inflammation, 2) administered FM-MSCs decreased Th1 and Th17 responses in EAM, 3) cultured FM-MSCs as well as BM-MSCs suppressed Th1 and Th17 differentiation from naïve CD4+ Th cells and 4) the expression of immunosuppressive molecules including IDO, IL-6, and HLA-G was increased in FM-MSC when they were co-cultured with Th17-polarized CD4+ T cells.

Myosin-induced EAM provides a model that resembles human giant cell myocarditis, consisting of an antigen priming phase from days 0 to 14, an autoimmune response phase from days 14 to 21, followed by a phase characterized by repair and fibrosis [21]. In rat EAM, Th immunity is thought to be responsible for disease pathogenesis induced by cardiac myosin immunization [8,22,23]. Published data suggest that the induction of EAM might be associated with Th1 dominance and recovery is related to Th2 polarity [8,22]. Recently, Th17 was reported to participate in cardiac inflammation in EAM [24]. Daniels et al. reported that Th17 as well as Th1 cells increase in number during the acute phase of EAM in A/J mice [24]. In addition, in mice lacking the T box transcription factor T-bet, required for Th1 differentiation, myocardial inflammation was more severe [25]. This knockout mouse showed a marked increase in production of

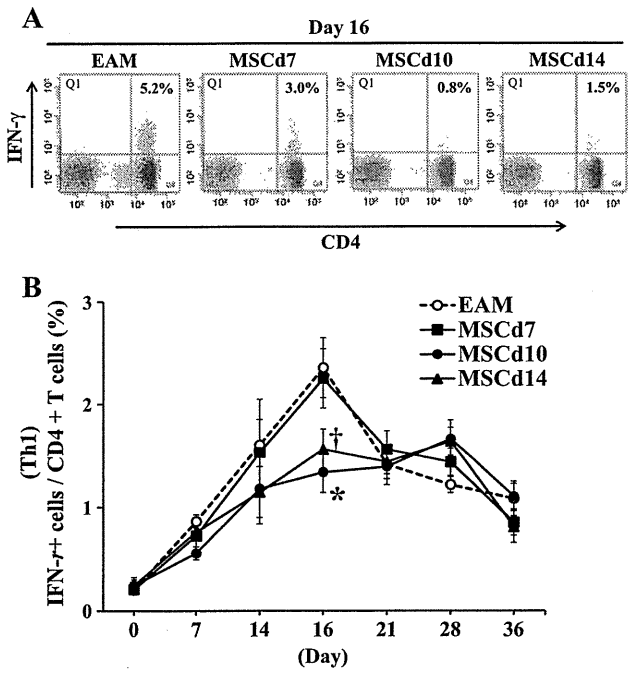

Fig. 3. Reduced induction of Th1 cells by allogenic FM-MSC administration in EAM rats. (A) Representative flow cytometric analysis of IFN-γ+/CD4+ T cells obtained from peripheral blood on day 16. (B) Time course of Th1 cell in myocarditis rats. The number of Th1 cells within CD4+ T cells increased after myosin administration, peaked at the stage of EAM (day 16), then gradually decreased. On day 16, FM-MSC administration significantly reduced Th1 cell induction in the MSCd10 and MSCd14 groups, compared to the untreated EAM group. *$P<0.05$ and **$P<0.01$ vs. EAM, n = 12–14.

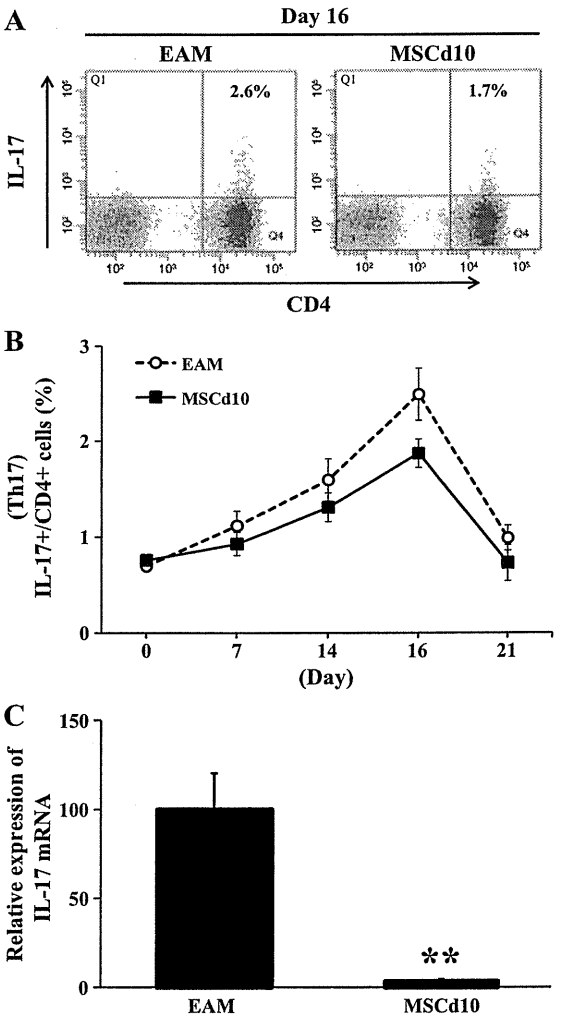

Fig. 4. Suppressed induction of Th17 cells by allogenic FM-MSC administration in EAM rats. (A) Representative flow cytometric analysis of peripheral IL-17+/CD4+ T cells on day 16. (B) Time course of Th17 cells in myocarditis rats. Th17 cells within CD4+ T cells increased after myosin administration, peaked at the stage of EAM (day 16), and decreased on day 21. FM-MSC administration significantly reduced Th17 cell induction in the MSCd10 group compared to the untreated EAM group. *$P<0.05$ vs. EAM, analyzed by two-way repeated measures ANOVA, n = 7. (C) IL-17 mRNA expression in the spleen of myocarditis rats on day 16. Quantitative RT-PCR analysis demonstrated that FM-MSC administration significantly decreased IL-17 gene expression. **$P<0.01$ vs. EAM, n = 7.

the IL-23-dependent cytokine IL-17 by heart-infiltrating lymphocytes. In vivo IL-17 depletion markedly reduced EAM severity in T-bet knockout mice. Since Th17 is credited with causing cardiac inflammation in EAM, we elected to examine the role of Th17 cells in the pathogenesis of EAM.

In our previous study, we demonstrated that intravenous administration of autologous BM-MSCs significantly improved cardiac function and myocardial inflammation in rats with EAM [13]. Since, in a clinical setting, the BM aspiration procedure is invasive, and a long period of expansion is required to obtain adequate numbers of BM-MSC, we focused on FMs, which are generally discarded as medical waste and possess great advantages due to their abundance and easy accessibility, as an alternative source of MSCs. Although FM-MSC administration implies allogenic transplantation, injection of allogenic rat FM-MSCs effectively attenuated myocardial injury in EAM rats [26]. Moreover, we confirmed that the allogenic human FM-MSCs as well as BM-MSCs similarly reduced human Th1 and Th17 cell-differentiation and proliferation.

Several groups have reported therapeutic effects of MSCs in various autoimmune disease models, including experimental autoimmune encephalomyelitis [27], collagen-induced arthritis [28], and EAM [12,13]. Previous reports, including ours, have focused on the differentiation potential or the paracrine activity of MSCs. We had thought that the therapeutic effects of MSCs in EAM were due to their differentiation into cardiovascular cells, or due to some angiogenic/proliferative property [13,29]. Although we previously reported that BM-MSC administration increased the number of capillaries in the cardiac tissue of EAM rats [13], no significant change in capillary density was observed in FM-MSC administered EAM rats [12], which might have been the result of differences in the angiogenic properties of BM-MSCs and FM-MSCs [12,13]. More importantly, the immune suppressive properties of MSCs have recently attracted increasing attention and seem to constitute a major mechanism through which MSCs provide therapeutic benefits [14,30,31]. In our recent study, we found that splenic T lymphocytes derived from FM-MSC-treated EAM rats demonstrated reduced proliferative activity compared to those from untreated EAM rats [26]. In addition, activated T cell proliferation was suppressed by co-culture with allogenic FM-MSC. These results indicate that allogenic FM-MSCs ameliorate myocardial damage in EAM by inhibiting T cell activation and proliferation, but the effects of transplanted MSCs on individual T cell effector pathways in the pathogenesis of EAM remain unclear.

To gain insight into the mechanism of disease improvement by FM-MSC administration, we examined the population of CD4+ Th cells [7]. Flow cytometric analysis demonstrated that circulating Th1/Th17 cells dominated during the inflammatory phase of disease, similar to previous reports [8,24]. Administration of allogenic FM-MSCs in EAM rats significantly reduced the numbers of circulating Th1 and Th17 cells in the inflammatory phase. Immunostaining of

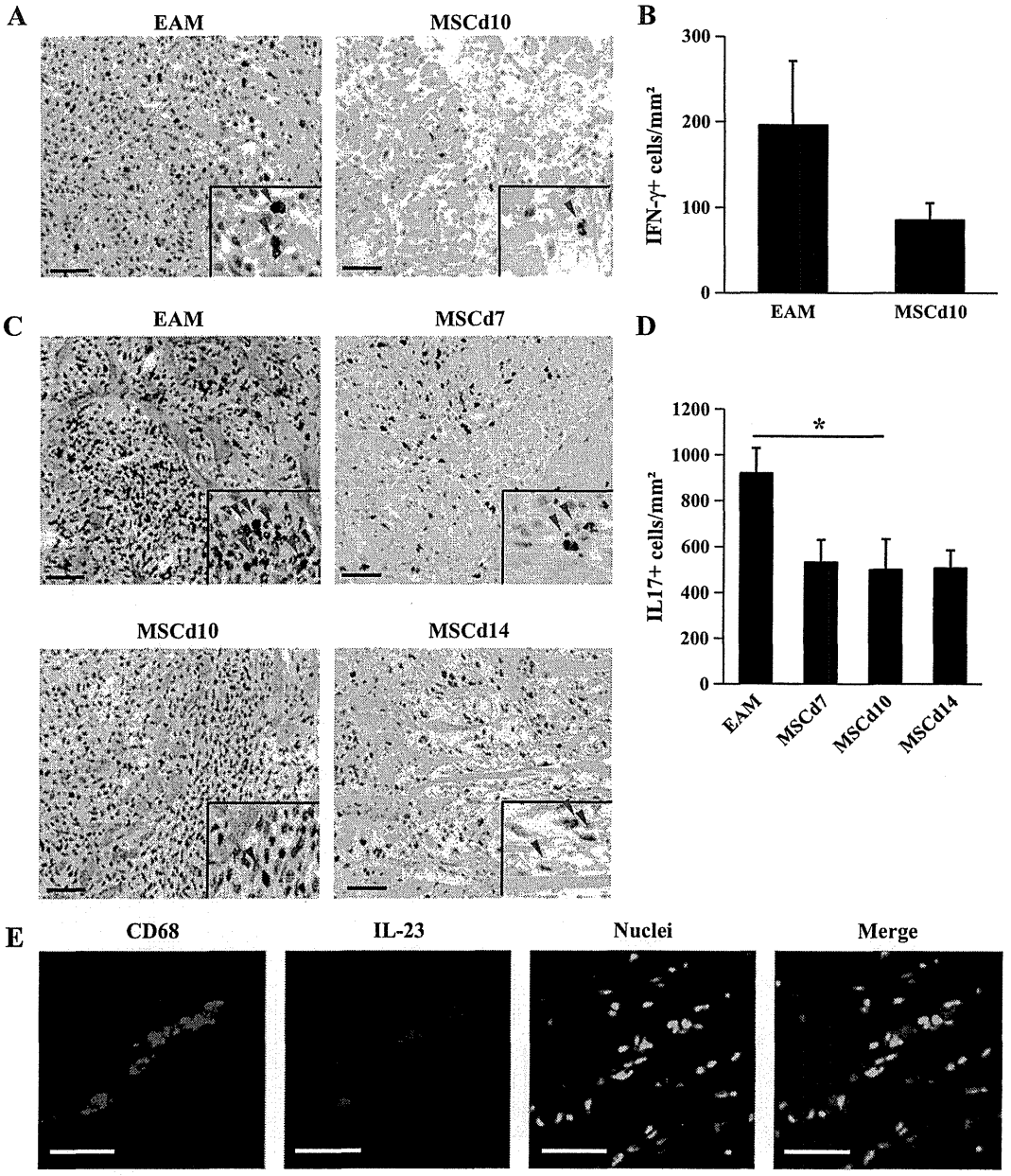

Fig. 5. Effects of FM-MSC administration on myocardial infiltration of IFN-γ+ and IL-17+ cells in EAM. (A, C) Representative immunohistological staining of IFN-γ+ cells (A, red arrow) and IL-17+ cells (B, red arrow). Scale bars: 50 μm. (B, D) Quantitative counts of IFN-γ+ (B) and IL-17+ (D) cells demonstrated that, compared to untreated EAM rats, FM-MSC administration significantly suppressed the infiltration of IL-17+ cells in the MSCd10 group (D), and a similar tendency was found for IFN-γ+ cells (B). *$P<0.05$ vs. EAM group, n=9–10. (E) Representative immunohistological staining of IL-23+ (blue) CD68+ (red) cells. Nuclei were stained with SYBR Green (green). In myocarditis tissue, all IL-23+ cells were entirely merged with CD68+ macrophages (merge). Scale bars: 50 μm.

heart tissues in the myocarditis phase revealed marked infiltration of IFN-γ- and IL-17-positive cells in EAM rats, and FM-MSC administration attenuated the number of IFN-γ/IL-17-positive cells. We also examined IFN-γ and IL-17 gene expression in the spleen and confirmed that FM-MSC administration significantly reduced the expression of IL-17, but not that of IFN-γ (data not shown). We also examined other Th subsets in EAM rats, but no significant changes in circulating Th2 or Treg cells were observed in FM-MSC-treated rats (data not shown). These results suggest that allogenic FM-MSCs ameliorate myocardial inflammation by suppressing the Th1/Th17 response.

Recent studies have indicated that BM-MSCs inhibit the development of a pro-inflammatory Th1 immune response [15]. In addition, BM-MSCs can inhibit Th17 cell differentiation and function [16,20]. To confirm whether FM-MSCs, as well as BM-MSCs, possess an inhibitory effect on Th1/17 cell differentiation, we performed an in vitro co-culture experiment. Similar to previous reports using BM-MSCs, we confirmed that human FM-MSCs markedly suppressed the proliferation of human CD4+ T cells and prevented their differentiation into both Th1 and Th17 cells. Recent studies have demonstrated that MSCs exert their immunosuppressive properties through the release of soluble factors including IDO2, IL-6, and soluble HLA-G5 [14,32–34]. We demonstrated that gene expression of IDO2, IL-6, and HLA-G in FM-MSCs was markedly increased when co-cultured with Th17-polarized CD4+ T cells. Therefore, these immunosuppressive factors secreted from FM-MSCs might suppress Th17 proliferation and differentiation.

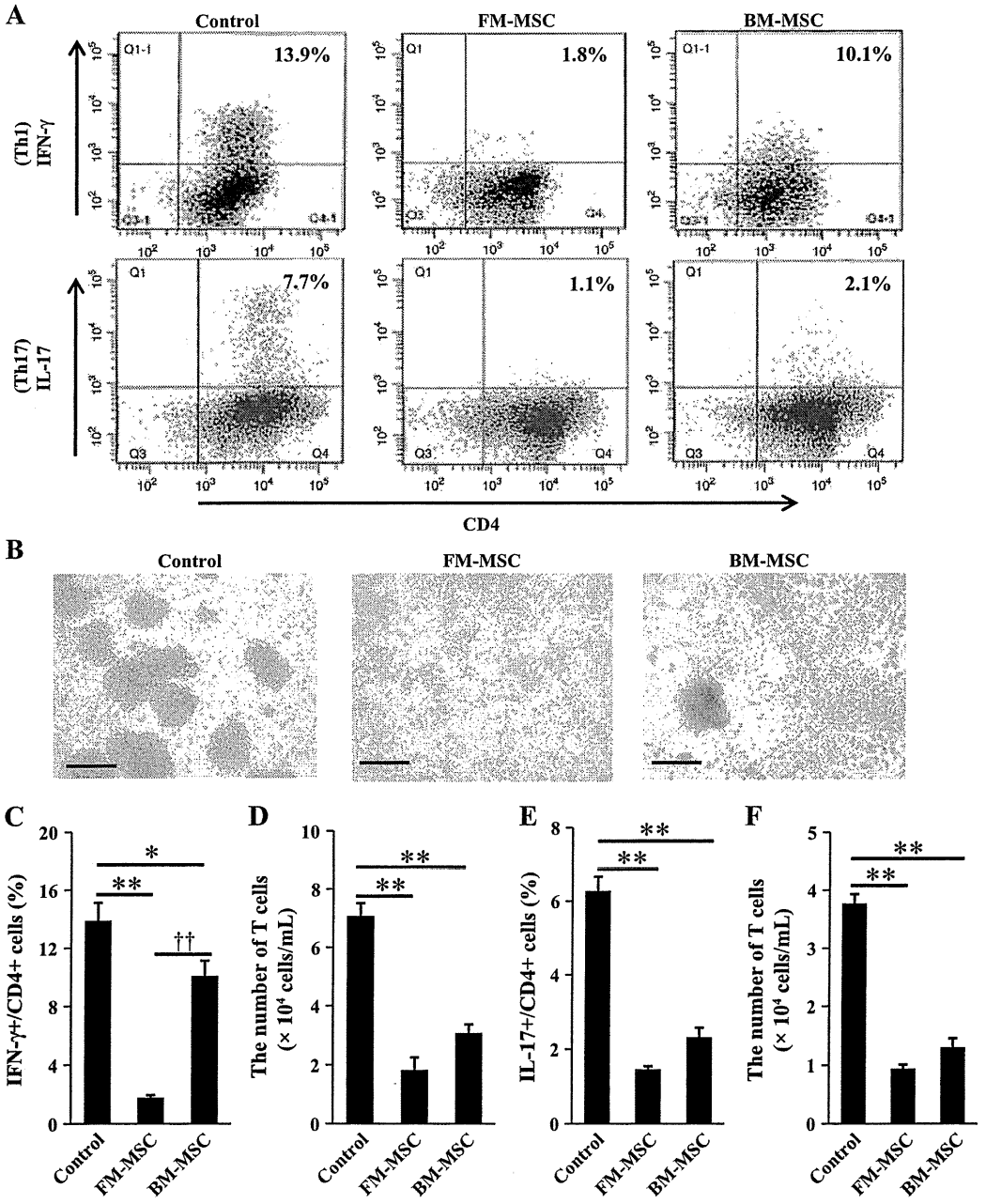

Fig. 6. Inhibition of Th1/Th17 proliferation and differentiation upon co-culture with BM-MSCs and FM-MSCs. (A) Representative flow cytometry plots of IFN-γ+/CD4+ and IL-17+/CD4+ T cells without MSC co-culture (control), with FM-MSC or BM-MSC co-culture. (B) Representative images of cultured CD4+ T cells without MSCs (control), with FM-MSCs or BM-MSCs under the Th17 inducing condition. (C, D) The percentage of Th1 cells within CD4+ T cells (C) and the number of proliferated T cells (D) after five days of co-culture with MSCs. Both FM-MSCs and BM-MSCs significantly inhibited the differentiation of Th1 cells and CD4+ T cell proliferation. FM-MSCs compared to BM-MSC, significantly inhibit the differentiation of Th1 cells. $^{*}P<0.05$ and $^{**}P<0.01$ vs. control, $\dagger\dagger P<0.01$: FM-MSC vs. BM-MSC, n=5. (E, F) The percentage of Th17 cells within CD4+ T cells (E) and the number of proliferated T cells (F) after five days of co-culture with MSCs. Both FM-MSCs and BM-MSCs significantly suppressed Th17 differentiation and T cell proliferation. $^{**}P<0.01$ vs. control, n=7.

In this study, we also investigated the optimal timing of FM-MSC transplantation in rats with EAM. We previously reported that a significant number of allogenic FM-MSCs could be detected 24 h after intravenous administration, but only a few FM-MSCs survived after 7 days and no FM-MSC were detected after 21 days [35]. Therefore, we considered that intravenously administered FM-MSCs would not survive for more than a week and speculated that there was an optimal time point to achieve the best therapeutic outcome when using FM-MSC transplantation. FM-MSCs injected intravenously at days 10 and 14 after myosin injection significantly improved cardiac function and suppressed the Th1/Th17 response, while FM-MSCs administered at day 7 showed a reduced therapeutic effect on myocarditis. This result might indicate that, because intravenously administered FM-MSCs survive only for a week, administration of FM-MSCs at day 7 might be too early to suppress the helper T cell response and myocarditis, and timing of FM-MSC administration is an important factor regulating Th1/Th17 immunity. However, Zappia et al. reported that MSC transplantation at day 3 and day 8 before disease onset, as well as at day 15 at the peak of disease, was effective in treating experimental autoimmune encephalomyelitis [27]. The reduced immunosuppressive

potential of FM-MSC with early administration in our EAM model may involve non-Th1/Th17 effects of FM-MSCs.

We have previously demonstrated that both allogenic FM-MSC and autologous BM-MSC transplantation in EAM attenuate heart-infiltrating monocytes/macrophages as well as cardiac monocyte chemoattractant protein-1 (MCP-1) expression [12,13]. Muggini et al. reported that MSCs directly induce activated macrophages to acquire a regulatory profile characterized by a reduced ability to produce inflammatory cytokines [36]. Since the inflammatory cells observed in myocardial lesions consist of 80% monocytes and macrophages [37] and blockade of MCP-1 significantly reduces macrophage infiltration and the severity of EAM [38], FM-MSC administration might directly suppress activated monocytes/macrophages in myocardial tissue. Interestingly, we found that infiltrated CD68-positive macrophages in cardiac tissue secreted IL-23, which is required for full acquisition of the function and maintenance of Th17 cells [39]. Therefore, in EAM, IL-23 secreted from activated macrophages in myocardial tissue might accelerate Th17 cell differentiation and function, which would worsen the disease outcome.

In conclusion, the results described in this study demonstrate the protective effects of intravenously administered FM-MSCs in EAM due to profound suppression of Th1/Th17 cells. Because FM-MSCs are available non-invasively in large numbers, these findings might provide a new perspective for the treatment of acute myocarditis.

Disclosures

None.

References

[1] Kodama M, Matsumoto Y, Fujiwara M. In vivo lymphocyte-mediated myocardial injuries demonstrated by adoptive transfer of experimental autoimmune myocarditis. Circulation 1992;85:1918–26.

[2] Kodama M, Zhang S, Hanawa H, Shibata A. Immunohistochemical characterization of infiltrating mononuclear cells in the rat heart with experimental autoimmune giant cell myocarditis. Clin Exp Immunol 1992;90:330–5.

[3] Hanawa H, Tsuchida M, Matsumoto Y, Watanabe H, Abo T, Sekikawa H, et al. Characterization of T cells infiltrating the heart in rats with experimental autoimmune myocarditis. Their similarity to extrathymic T cells in mice and the site of proliferation. J Immunol 1993;150:5682–95.

[4] Palaniyandi SS, Watanabe K, Ma M, Tachikawa H, Kodama M, Aizawa Y. Inhibition of mast cells by interleukin-10 gene transfer contributes to protection against acute myocarditis in rats. Eur J Immunol 2004;34:3508–15.

[5] Kodama M, Matsumoto Y, Fujiwara M, Masani F, Izumi T, Shibata A. A novel experimental model of giant cell myocarditis induced in rats by immunization with cardiac myosin fraction. Clin Immunol Immunopathol 1990;57:250–62.

[6] Kodama M, Matsumoto Y, Fujiwara M, Zhang SS, Hanawa H, Itoh E, et al. Characteristics of giant cells and factors related to the formation of giant cells in myocarditis. Circ Res 1991;69:1042–50.

[7] Okura Y, Takeda K, Honda S, Hanawa H, Watanabe H, Kodama M, et al. Recombinant murine interleukin-12 facilitates induction of cardiac myosin-specific type 1 helper T cells in rats. Circ Res 1998;82:1035–42.

[8] Fuse K, Kodama M, Ito M, Okura Y, Kato K, Hanawa H, et al. Polarity of helper T cell subsets represents disease nature and clinical course of experimental autoimmune myocarditis in rats. Clin Exp Immunol 2003;134:403–8.

[9] Fuse K, Kodama M, Aizawa Y, Yamaura M, Tanabe Y, Takahashi K, et al. Th1/Th2 balance alteration in the clinical course of a patient with acute viral myocarditis. Jpn Circ J 2001;65:1082–4.

[10] Cruz-Adalia A, Jimenez-Borreguero LJ, Ramirez-Huesca M, Chico-Calero I, Barreiro O, Lopez-Conesa E, et al. CD69 limits the severity of cardiomyopathy after autoimmune myocarditis. Circulation 2010;122:1396–404.

[11] Valaperti A, Marty RR, Kania G, Germano D, Mauermann N, Dirnhofer S, et al. CD11b+ monocytes abrogate Th17 CD4+ T cell-mediated experimental autoimmune myocarditis. J Immunol 2008;180:2686–95.

[12] Ishikane S, Yamahara K, Sada M, Harada K, Kodama M, Ishibashi-Ueda H, et al. Allogeneic administration of fetal membrane-derived mesenchymal stem cells attenuates acute myocarditis in rats. J Mol Cell Cardiol 2010;49:753–61.

[13] Ohnishi S, Yanagawa B, Tanaka K, Miyahara Y, Obata H, Kataoka M, et al. Transplantation of mesenchymal stem cells attenuates myocardial injury and dysfunction in a rat model of acute myocarditis. J Mol Cell Cardiol 2007;42:88–97.

[14] Uccelli A, Moretta L, Pistoia V. Mesenchymal stem cells in health and disease. Nat Rev Immunol 2008;8:726–36.

[15] Aggarwal S, Pittenger MF. Human mesenchymal stem cells modulate allogeneic immune cell responses. Blood 2005;105:1815–22.

[16] Duffy MM, Pindjakova J, Hanley SA, McCarthy C, Weidhofer GA, Sweeney EM, et al. Mesenchymal stem cell inhibition of T-helper 17 cell differentiation is triggered by cell-cell contact and mediated by prostaglandin E2 via the EP4 receptor. Eur J Immunol 2011;41:2840–51.

[17] Kodama M, Fujiwara M, Masani F, Izumi T, Shibata A. A novel experimental model of giant cell myocarditis induced in rats by immunization with cardiac myosin fraction. Clin Immunol Immunopathol 1990;57:250–62.

[18] Openshaw P, Murphy EE, Hosken NA, Maino V, Davis K, Murphy K, et al. Heterogeneity of intracellular cytokine synthesis at the single-cell level in polarized T helper 1 and T helper 2 populations. J Exp Med 1995;182:1357–67.

[19] Ljungdahl A, Olsson T, Van der Meide PH, Holmdahl R, Klareskog L, Hojeberg B. Interferon-gamma-like immunoreactivity in certain neurons of the central and peripheral nervous system. J Neurosci Res 1989;24:451–6.

[20] Ghannam S, Pene J, Torcy-Moquet G, Jorgensen C, Yssel H. Mesenchymal stem cells inhibit human Th17 cell differentiation and function and induce a T regulatory cell phenotype. J Immunol 2010;185:302–12.

[21] Kodama M, Hanawa H, Saeki M, Hosono H, Inomata T, Suzuki K, et al. Rat dilated cardiomyopathy after autoimmune giant cell myocarditis. Circ Res 1994;75:278–84.

[22] Cunningham MW. Cardiac myosin and the TH1/TH2 paradigm in autoimmune myocarditis. Am J Pathol 2001;159:5–12.

[23] Smith SC, Allen PM. Myosin-induced acute myocarditis is a T cell-mediated disease. J Immunol 1991;147:2141–7.

[24] Daniels MD, Hyland KV, Wang K, Engman DM. Recombinant cardiac myosin fragment induces experimental autoimmune myocarditis via activation of Th1 and Th17 immunity. Autoimmunity 2008;41:490–9.

[25] Rangachari M, Mauermann N, Marty RR, Dirnhofer S, Kurrer MO, Komnenovic V, et al. T-bet negatively regulates autoimmune myocarditis by suppressing local production of interleukin 17. J Exp Med 2006;203:2009–19.

[26] Ishikane S, Ohnishi S, Yamahara K, Sada M, Harada K, Mishima K, et al. Allogeneic injection of fetal membrane-derived mesenchymal stem cells induces therapeutic angiogenesis in a rat model of hind limb ischemia. Stem Cells 2008;26:2625–33.

[27] Zappia E, Casazza S, Pedemonte E, Benvenuto F, Bonanni I, Gerdoni E, et al. Mesenchymal stem cells ameliorate experimental autoimmune encephalomyelitis inducing T-cell anergy. Blood 2005;106:1755–61.

[28] Augello A, Tasso R, Negrini SM, Amateis A, Indiveri F, Cancedda R, et al. Bone marrow mesenchymal progenitor cells inhibit lymphocyte proliferation by activation of the programmed death 1 pathway. Eur J Immunol 2005;35:1482–90.

[29] Nagaya N, Kangawa K, Itoh T, Iwase T, Murakami S, Miyahara Y, et al. Transplantation of mesenchymal stem cells improves cardiac function in a rat model of dilated cardiomyopathy. Circulation 2005;112:1128–35.

[30] Griffin MD, Ritter T, Mahon BP. Immunological aspects of allogeneic mesenchymal stem cell therapies. Hum Gene Ther 2010;21:1641–55.

[31] English K, French A, Wood KJ. Mesenchymal stromal cells: facilitators of successful transplantation? Cell Stem Cell 2010;7:431–42.

[32] Jones BJ, Brooke G, Atkinson K, McTaggart SJ. Immunosuppression by placental indoleamine 2,3-dioxygenase: a role for mesenchymal stem cells. Placenta 2007;11–12:1174–81.

[33] Bouffi C, Bony C, Courties G, Jorgensen C, Noel D. IL-6-dependent PGE2 secretion by mesenchymal stem cells inhibits local inflammation in experimental arthritis. PLoS One 2010;5:e14247.

[34] Morandi F, Raffaghello L, Bianchi G, Meloni F, Salis A, Millo E, et al. Immunogenicity of human mesenchymal stem cells in HLA-class I-restricted T-cell responses against viral or tumor-associated antigens. Stem Cells 2008;26:1275–87.

[35] Tsuda H, Yamahara K, Ishikane S, Otani K, Nakamura A, Sawai K, et al. Allogenic fetal membrane-derived mesenchymal stem cells contribute to renal repair in experimental glomerulonephritis. Am J Physiol Renal Physiol 2010;299:F1004–13.

[36] Maggini J, Mirkin G, Bognanni I, Holmberg J, Piazzon IM, Nepomnaschy I, et al. Mouse bone marrow-derived mesenchymal stromal cells turn activated macrophages into a regulatory-like profile. PLoS One 2010;5:e9252.

[37] Pummerer C, Berger P, Fruhwirth M, Ofner C, Neu N. Cellular infiltrate, major histocompatibility antigen expression and immunopathogenic mechanisms in cardiac myosin-induced myocarditis. Lab Invest 1991;65:538–47.

[38] Goser S, Ottl R, Brodner A, Dengler TJ, Torzewski J, Egashira K, et al. Critical role for monocyte chemoattractant protein-1 and macrophage inflammatory protein-1alpha in induction of experimental autoimmune myocarditis and effective anti-monocyte chemoattractant protein-1 gene therapy. Circulation 2005;112:3400–7.

[39] Langrish CL, Chen Y, Blumenschein WM, Mattson J, Basham B, Sedgwick JD, et al. IL-23 drives a pathogenic T cell population that induces autoimmune inflammation. J Exp Med 2005;201:233–40.

Cytotherapy, 2012; 14: 441–450

informa
healthcare

Human umbilical cord provides a significant source of unexpanded mesenchymal stromal cells

AKIE KIKUCHI-TAURA[1,2], AKIHIKO TAGUCHI[1], TAKAYOSHI KANDA[3], TAKAYUKI INOUE[2], YUKIKO KASAHARA[1], HARUKA HIROSE[1], IORI SATO[2], TOMOHIRO MATSUYAMA[4], TAKAYUKI NAKAGOMI[4], KENICHI YAMAHARA[1], DAVID STERN[5], HIROYASU OGAWA[2] & TOSHIHIRO SOMA[2]

[1]*Department of Regenerative Medicine, National Cerebral and Cardiovascular Center, Osaka, Japan,* [2]*Division of Hematology, Department of Internal Medicine, Hyogo College of Medicine, Hyogo, Japan,* [3]*Department of Perinatal Medicine, Osaka Minami Medical Center, Osaka, Japan,* [4]*Institute for Advanced Medical Sciences, Hyogo College of Medicine, Hyogo, Japan, and* [5]*Executive Dean's Office, University of Tennessee, Tennessee, USA*

Abstract

Background aims. Human mesenchymal stromal cells (MSC) have considerable potential for cell-based therapies, including applications for regenerative medicine and immune suppression in graft-versus-host disease (GvHD). However, harvesting cells from the human body can cause iatrogenic disorders and *in vitro* expansion of MSC carries a risk of tumorigenesis and/or expansion of unexpected cell populations. *Methods.* Given these problems, we have focused on umbilical cord, a tissue obtained with few ethical problems that contains significant numbers of MSC. We have developed a modified method to isolate MSC from umbilical cord, and investigated their properties using flow cytometry, mRNA analysis and an *in vivo* GvHD model. *Results.* Our study demonstrates that, using umbilical cord, large numbers of MSC can be safely obtained using a simple procedure without *in vitro* expansion, and these non-expanded MSC have the potential to suppress GvHD. *Conclusions.* Our results suggest that the combined banking of umbilical cord-derived MSC and identical cord blood-derived hematopoietic stem cell banking, where strict inspection of the infectious disease status of donors is performed, as well as further benefits of HLA-matched mesenchymal cells, could become one of the main sources of cells for cell-based therapy against various disorders.

Key Words: *cell banking, graft-versus-host disease, mesenchymal stromal cells, umbilical cord*

Introduction

Mesenchymal stromal cells (MSC) can be obtained from various tissues, including bone marrow (1), adipose tissue (2), trabecular bone (3), synovium (4), pancreas (5), lung, liver, spleen (6), peripheral blood (7), cord blood (8), amniotic fluid and umbilical cord (9–11). MSC include multiple cell types that have the capacity to differentiate into neurons, adipocytes, cartilage, skeletal muscle, hepatocytes and cardiomyocytes, under appropriate conditions across embryonic germ layers (2,12). Cell-based therapies using MSC have been initiated in patients with arthrosis (13), corneal disorders (14), stroke (15) and chronic heart failure (16). MSC are also used to suppress graft-versus-host disease (GvHD) in patients after allogeneic hematopoietic stem cell transplantation, and co-transplantation of hematopoietic cells and MSC to enhance engraftment has provided promising results (17). To broaden the indications for use of MSC against multiple disorders, cell banking with HLA-typing would be desirable.

Although MSC can be obtained from a range of organs, the iatrogenic risks associated with harvesting cells from the human body cannot be denied, particularly with harvesting from the large number of individuals required to establish a cell bank. In contrast, harvesting of cells from umbilical cord carries little risk to the donor, and MSC have been identified in placenta (18), amniotic fluid (19), umbilical cord blood (20) and the umbilical cord itself (21). Furthermore, the omission of *in vitro* expansion offers significant benefits for cell banks with large numbers of samples. The present study focused on the umbilical cord, because of the relative ease of cleaning the tissue before harvest and subsequent isolation of the cells. The umbilical cord is covered by

Correspondence: **Akihiko Taguchi,** Department of Regenerative Medicine, National Cerebral and Cardiovascular Center, 5-7-1 Fujishiro-dai, Suita, Osaka, Japan 565–8565. E-mail: taguchi@ri.ncvc.go.jp

(Received 2 June 2011; accepted 13 January 2012)

ISSN 1465-3249 print/ISSN 1477-2566 online
DOI: 10.3109/14653249.2012.658911

an epithelium derived from the enveloping amnion and contains two arteries and one vein, all of which are surrounded by the mucoid connective tissue of Wharton's jelly. The main role of this jelly-like material is to prevent compression, torsion and bending of the enclosed vessels, which provide bidirectional blood flow between the fetal and maternal circulations. The network of glycoprotein microfibrils and collagen fibrils in Wharton's jelly has already been elucidated (22). The phenotypic stromal cells in Wharton's jelly are fibroblast-like cells (23), morphologically and immunophenotypically similar to MSC isolated from bone marrow (9,24,25). MSC from the umbilical cord have been shown to differentiate into adipocytes, osteocytes, neurons and insulin-producing cells (9,24–30). Carlin *et al.* (31) recently demonstrated embryonic transcription factors, such as octamer-binding transcription factor (Oct)-4, sex determining region Y-box (Sox)-2 and Nanog, in porcine umbilical cord matrix cells. These results indicate that umbilical cord-derived mesenchymal stem (UCMS) cells may represent a major source of cells for cell-based therapy. The present study demonstrates that large numbers of MSC can be obtained from umbilical cord using a simple procedure without *in vitro* expansion. Furthermore, UCMS isolated using this procedure are shown to suppress severe GvHD in a murine model.

Methods

All procedures for the isolation and differentiation of human UCMS cells were approved by the Osaka Minami Medical Center (Osaka, Japan). institutional review board and all volunteer donating mothers provided written informed consent. Animal experiments were carried out in accordance with the guidelines of the Animal Care Committee of Hyogo College of Medicine (Hyogo, Japan). Quantitative analyzes were conducted by an investigator who had been blinded to the experimental protocol, identities of animals and experimental conditions pertaining to the animals under study.

Isolation of UCMS cells

Human umbilical cords were obtained from patients delivered at full-term by Cesarean section ($n = 30$). After collection of cord blood as described previously (32), placenta and umbilical cord were placed into a sterilized bag and the following procedures were performed in a safety cabinet. In this study, we used only umbilical cord tissue for further experiments. Both ends of the umbilical cord (approximately 1 cm from each end) were cut and discarded with the placenta. The remaining umbilical cord was immersed and washed in 80% ethanol for 1 min, rinsed with sterile saline twice and cut into approximately 10-cm lengths. Cord blood and blood clots in the umbilical cord artery were removed by flushing twice, using a 20-G tip cut needle, sterile saline and 20-mL syringe. Then the umbilical cord segments were immersed and washed with 80% ethanol for 1 min, followed by two rinses with sterile saline. Next, the umbilical cord was cut into 2–4-cm lengths and the epithelial tissue was removed using sterilized scissors. The remaining tissue was incubated in an enzyme cocktail solution, containing 1 mg/mL hyaluronidase (Sigma-Aldrich, St Louis, MO, USA), 300 U/mL collagenase (Sigma-Aldrich) and 3 mM $CaCl_2$ (Wako Pure Chemical Industries, Osaka, Japan) in Dulbecco's modified Eagle's medium (DMEM) (Invitrogen, Carlsbad, CA, USA) for 2 h at 37°C with shaking (50 shakes/min; BR-21UM; Taitec, Saitama, Japan). After incubation, undigested vascular components were removed and the tissue solution was crushed with forceps and passed through 180- and 125-μm diameter stainless steel mesh (Tokyo Screen, Tokyo, Japan), followed by 70-μm diameter mesh (Becton Dickinson, Franklin Lakes, NJ, USA), to remove large pieces of unlysed tissue. The tissue solution was then collected by centrifugation (200 ***g*** for 5 min) and resuspended in phosphate-buffered saline (PBS). The latter washing procedure was performed twice. Next, the tissue solution was incubated with 0.5% trypsin–ethylenediamine tetraacetic acid. (EDTA) (Invitrogen) in PBS for 1 h at 37°C. After trypsinization, the tissue solution was neutralized with 2% fetal bovine serum (FBS) in DMEM and this washing procedure was performed twice. As a control, the conventional method of tissue preparation reported by Weiss *et al.* (29) was used to isolate UCMS cells. That procedure is similar to our own, the major difference being that we did not remove the umbilical artery from the umbilical cord before digestion with hyaluronidase and collagenase.

Flow cytometric analysis of UCMS cells

Antigens expressed by freshly isolated and *in vitro*-expanded and -differentiated umbilical cord-derived cells were investigated by multicolor flow cytometry. The expression of surface markers in 1×10^5 cells was analyzed. The characteristics of each antibody are listed in Table I. As a control, a non-immune isotype control (Beckman Coulter Orange County, CA, USA) was employed.

Expansion and in vitro *differentiation of UCMS cells*

To investigate the properties of isolated UCMS cells as MSC, cells were expanded *in vitro* as described previously (29). Briefly, 1×10^4 cells/cm^2 were plated in a low-serum media, containing 56% low-glucose DMEM (Invitrogen), 37% MCDB201

Table I. Antibodies for flow cytometry.

Antigen	Label	Manufacturer	Catalog number
CD11b	FITC	Beckman Coulter	IM1284
CD14	FITC	Beckman Coulter	IM0645
CD19	FITC	Beckman Coulter	IM1284
CD29	FITC	Beckman Coulter	6604105
CD31	FITC	BD	555445
CD34	PC7	Beckman Coulter	A21691
CD34	PC5	Beckman Coulter	A07777
CD38	FITC	Beckman Coulter	IM0775
CD44	PE[a]	Beckman Coulter	IM0845
CD45	FITC	Beckman Coulter	A07782
CD45	ECD	Beckman Coulter	A07784
CD73	Biotin[b]	BD	550256
CD90	PE	Beckman Coulter	IM1840
CD105	PE	Beckman Coulter	A07414
CD117	PE	Beckman Coulter	IM2732
CD133	PE	Miltenyi Biotec	130-080-901
GlycophorinA	PE	Beckman Coulter	IM2211
HLA-DR	FITC	BD	555560
vWF	FITC*	Beckman Coulter	IM0150

[a]Antibody was labeled with a Zenon Mouse IgG1 labeling kit (Invitrogen).
[b]Biotin-labeled antibody was detected by strept avidin-PC5.
FITC, fluorescein isothiocyanate; PE, phycoerythrin; PC, phycoerythrin-cyanin; ECD, phycoerythrin-TexasRED. BD, Becton Dickinson, Franklin Lakes, NJ, USA, Mitenyi Biotec; Bergisch Gladbach, Nordrhein-Westfalen, Germany

(Sigma-Aldrich), 2% FBS (StemCell Technologies, Vancouver, Canada), 1 × insulin-transferrin-selenium-X (ITS-X; Invitrogen), 1 × ALBU-Max I (Invitrogen), 1 × antibiotics-antimycotics (Invitrogen), 10 nM dexamethasone (Sigma-Aldrich), 50 μM ascorbic acid 2-phosphate (Sigma-Aldrich), 1 ng/mL epidermal growth factor (EGF; Peprotech, Rocky Hill, NJ, USA) and 10 ng/mL platelet-derived growth factor-BB (PDGF-BB; (R&D Systems, Minneapolis, MN, USA). After reaching 70–80% confluence, cells were replated at 20% confluence.

After cell expansion (passage 2), 70% confluent UCMS cells were differentiated into neuronal cells, adipocytes, osteocytes, chondrocytes, myoblasts, and pancreatic cells, as described previously (33–36). Briefly, prior to neuronal induction, UCMS cells were grown overnight in DMEM with 20% FBS (Invitrogen) and 10 ng/mL basic fibroblast growth factor (Peprotech). Cells were rinsed twice with PBS and incubated in DMEM with 100 μM butylated hydroxyanisole (BHA; Sigma-Aldrich), 10 μM forskolin (Sigma-Aldrich), 2% dimethyl sulfoxide (DMSO; Sigma-Aldrich), 5 U/mL heparin (Fuso Pharmaceutical Industries, Osaka, Japan), 5 nM K252a (Sigma-Aldrich), 25 mM KCl (Wako Pure Chemical Industries), 2 mM valproic acid (Sigma-Aldrich) and 1 × N2 supplement (Invitrogen). For differentiation into adipocytes, UCMS cells were incubated in DMEM with 1 μM dexamethasone, 0.5 mM 3-isobutyl-1-methlxanthine (Sigma-Aldrich), 1 μg/mL insulin (Sigma-Aldrich) and 100 μM indomethacin (Sigma-Aldrich). Differentiated cells were stained with Oil Red O (Sigma-Aldrich). For differentiation into osteocytes, UCMS cells were incubated in osteogenic differentiation medium in accordance with the manufacturer's protocol for 31 days (Invitrogen). Differentiated cells were stained with Alizarin Red S (Sigma-Aldrich). To investigate the potential formation of a chondrogenic pellet, UCMS cells were incubated in chondrogenic differentiation medium according to the manufacturer's protocol for 21 days (Invitrogen). Differentiated cell pellets were stained with Alcian Blue (Sigma-Aldrich) and cross-sections were studied. For differentiation into myoblasts, UCMS cells were initially incubated in DMEM with 2% FBS, 10 ng/mL EGF, 10 ng/mL PDGF-BB and 3 μM 5-azacytidine (Sigma-Aldrich) for 24 h. The medium was then changed to DMEM with 2% FBS, 10 ng/mL EGF and 10 ng/mL PDGF-BB. For differentiation into pancreatic cells, UCMS cells were cultured for 7 days in RPMI-1640 medium (Sigma-Aldrich) with 5% FBS and 10 mmol/L nicotinamide (Sigma-Aldrich). Cells were then cultured for an additional 5 days in the presence of 10 nM exendin 4 (Sigma-Aldrich).

Total RNA extraction and reverse transcriptase–polymerase chain reaction analysis

Total RNA was extracted from freshly isolated and *in vitro*-differentiated UCMS cells using RNeasy purification reagent (Qiagen, Hilden, Germany). Reverse transcriptase–polymerase chain reaction (RT-PCR) analysis was performed using a SuperScript One-Step RT-PCR System (Invitrogen) with 100 ng of tRNA. Sequences and annealing temperatures for each primer are described in Table II. The amplified cDNA was separated by electrophoresis through a 2% agarose gel, stained with ethidium bromide, and photographed under ultraviolet light.

GvHD model

Female B6C3F1 (recipient; C57BL/6 × C3H/He; H-$2^{b/k}$) and BDF1 (donor; C57BL/6 × DBA/2; H-$2^{b/d}$) mice between 8 and 12 weeks old were purchased from Japan SLC (Shizuoka, Japan). Mice were housed in sterile micro-isolator cages in a pathogen-free facility with *ad libitum* access to autoclaved food and hyperchlorinated drinking water. Donor bone marrow cells were harvested from tibiae and femurs by flushing with RPMI-1640 medium (Sigma-Aldrich). Recipient mice were lethally irradiated with 13 Gy total body irradiation (TBI; X-ray) split into two doses separated by 3 h. This amount of radiation and dose of infused donor cells has been shown to

Table II. Sequence of RT-PCR primers.

Gene	5′-primer	3′-primer	Temp. (°C)
Osteopontin	CTAGGCATCACCTGTGCCATACC	CAGTGACCAGTTCATCAGATTCATC	60
ALP	TCAGAAGCTCAACACCAACG	GTCAGGGACCTGGGCATT	51
Sox-9	ACATCTCCCCCAACGCCATC	TCGCTTCAGGTCAGCCTTGC	51
Aggrecan	TGCGGGTCAACAGTGCCTATC	CACGATGCCTTTCACCACGAC	51
PPARγ2	GCATTATGAGACATCCCCACTGC	CCTATTGACCCAGAAAGCGATTC	59
GFAP	CTGGGCTCAAGCAGTCTACC	AATTGCCTCCTCCTCCATCT	58
MAP-2	CTGCTTTACAGGGTAGCACAA	TTGAGTATGGCAAACGGTCTG	58
MyoD	GCTAGGTTCACGTTTCTCGC	GCGCCTTTATTTTGATCACC	58
Glucagon	GAGGGCTTGCTCTCTCTTCA	GTGAATGTGCCCTGTGAATG	57

ALP, alkaline phosphatase; GFAP, glial fibrillary acidic protein; MAP, microtubule-associated protein PPAR, peroxisome proliferator-activated receptor..

induce GvHD after hematopoietic stem cell transplantation (37). On the following day, donor-derived cells (1×10^7 bone marrow cells and 2×10^7 spleen cells) were suspended in 0.2 mL RPMI-1640 medium and transplanted via the tail vein into post-irradiation recipient mice. Soon after hematopoietic stem cell transplantation, 1×10^6 non-expanded and non-selected UCMS cells in 0.2 mL RPMI medium were transplanted via the tail vein. In the control group, the same amount of RPMI was infused via the tail vein. On day 7 after transplantation, the same number of non-expanded UCMS cells or RPMI medium alone was injected via the tail vein into treated mice or control mice, respectively. The severity of GvHD was evaluated using a scoring system incorporating five clinical parameters, as described previously (38): body weight; posture (hunching); mobility; fur texture; and skin integrity. Mice were evaluated and graded from 0 to 2 for each criterion. A clinical index was subsequently generated by summation of the five criteria scores (38). A score of 0–5 was defined as mild GvHD and a score of 6–10 or dead was defined as severe GvHD.

Statistical analysis

Statistical comparisons were performed using a Student's *t*-test or χ^2 test. For all experiments,

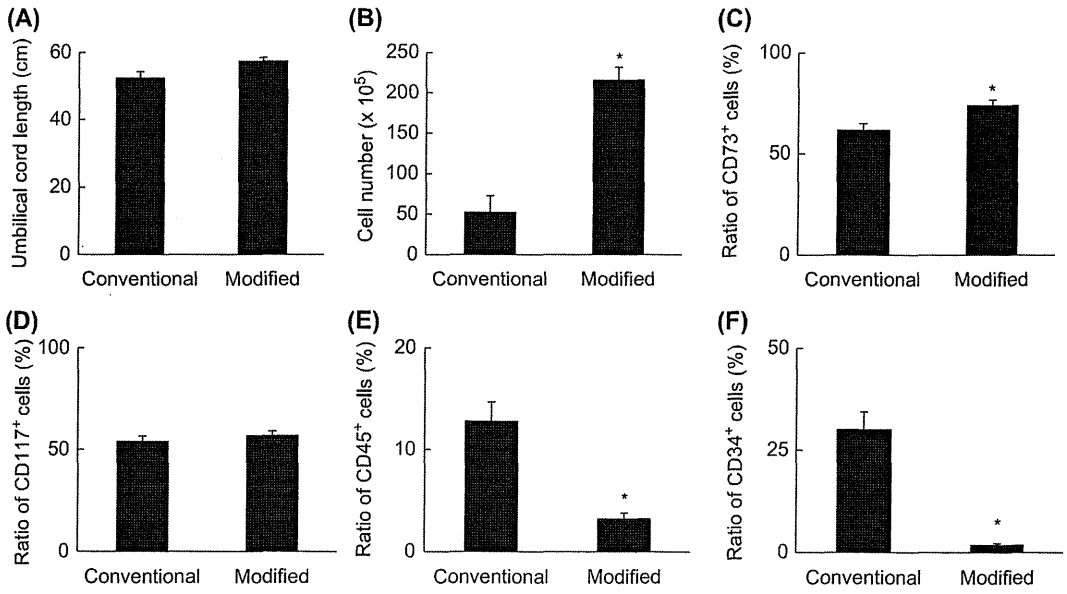

Figure 1. Cell numbers and characteristics of isolated MSC. No significant difference in the length of the umbilical cord was seen between groups (A). The total number of cells obtained with our modified method (216×10^5 cells) was more than 4-fold greater, compared with the conventional method (52×10^5 cells) (B). A significant increase in the ratio of cells expressing an MSC marker (CD73) was observed with the modified method (74.1%), compared with the conventional method (61.8%) (C). In contrast, no significant difference was observed in CD117-positive cells between modified (56.9%) and conventional methods (54.1%) (D). Contamination by cells from the hematopoietic lineage, expressing CD45 (E) and CD34 (F), was significantly decreased with the modified method (3.2% and 1.9%, respectively), compared with the conventional method (12.8% and 30.1%, respectively). *$P < 0.05$ versus conventional method.

values are reported as mean ± standard error of the mean. Values of $P < 0.05$ were considered statistically significant.

Results

Characterization of isolated UCMS cells

MSC were isolated from umbilical cord using either conventional methods (29) ($n = 12$) or our modified methodology ($n = 18$). Although no significant differences in the length of umbilical cords were observed (Figure 1A), more than four times as many cells were obtained using our method (Figure 1B). To investigate the characteristics of these cells, surface cell markers were analyzed by flow cytometry for CD73, as an MSC marker (Figure 1C); a significant increase in the ratio of CD73-positive MSC was observed using our method, compared with the conventional technique. In contrast, no significant difference in the ratio of cells positive for the stem cell marker CD117 was identified between groups (Figure 1D). Umbilical cord contains a range of cell types, including hemocytes and endothelial cells. To investigate the level of these cells in our final cell population, numbers of CD45- and CD34-positive cells were investigated by flow cytometry (CD45, Figure 1E; CD34, Figure 1F). We observed a significant reduction in contamination by endothelial cells using our modified methodology compared with the conventional technique.

To evaluate properties of freshly isolated umbilical cord-derived cells, cell surface markers were analyzed by multiple staining for cell-surface markers. As shown in Figure 2, only a small fraction of CD73-positive cells displayed hemocyte/hematopoietic cell markers, including anti-CD11b, CD14, CD19, CD34, CD38, CD45, CD133, GlycophorinA and HLA-DR. These results indicated that the CD73-positive cell fraction contained a low level of hemocyte or hematopoietic cells. To evaluate the presence of endothelial cells in the CD73-positive cell fraction, the expression of various endothelial cell markers, including CD31, CD34 and von Willebrand Factor (vWF), was investigated; the majority of CD73-positive cells were negative for these endothelial cell markers. To confirm our results, expression of CD90, a marker not present on endothelial cells (39), was evaluated; more than 95% of CD73-positive cells expressed CD90. These findings indicated little contamination by endothelial cells using our modified methodology and were consistent with the visual impression that most vascular components remained undigested after incubation with hyaluronidase and collagenase for 2 h.

Changes in cell-surface markers of isolated umbilical cord-derived cells after in vitro expansion

To evaluate further the character of the isolated cell population, freshly prepared umbilical cord-derived cells using our modified methodology were cultured up to passage 4. Expanded cells showed a spindle-shaped morphology (Figure 3A) that associated with common MSC. Analysis of cell-surface markers revealed that expression of CD44 (Figure 3B; a cell-surface glycoprotein involved in cell–cell interactions expressed by mesenchymal cells), CD105 (Figure 3C; a membrane glycoprotein expressed

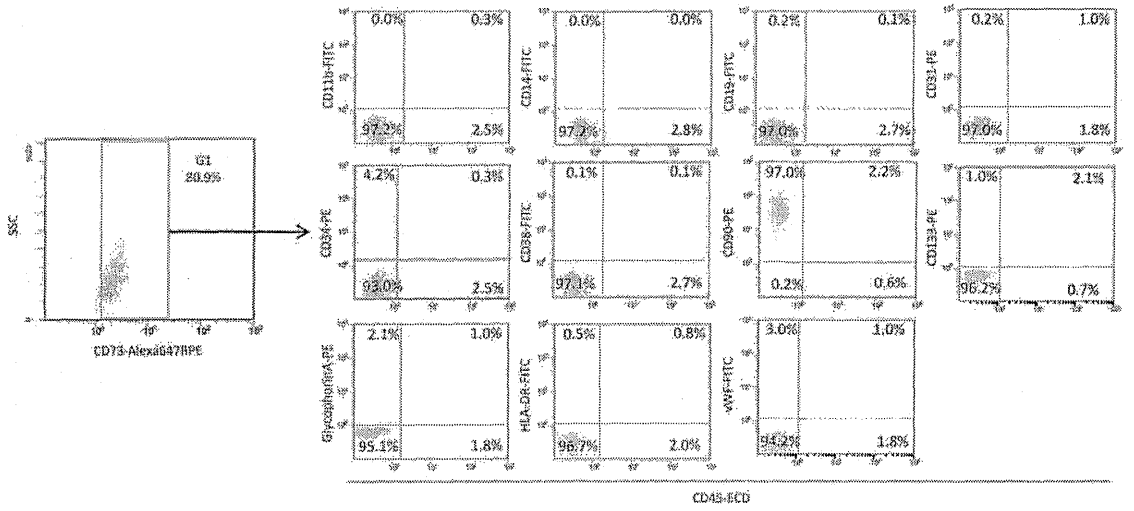

Figure 2. Multicolor analysis of freshly isolated MSC obtained by the modified protocol. To evaluate the presence of non-MSC, surface markers of freshly isolated cells were investigated. The majority of CD73-positive cells were negative for markers of hemocyte (CD11b, CD14, CD19, CD34, CD38, CD133, GlycophorinA, HLA-DR) and endothelial cell (CD31, vWF) lineages. It is notable that most of the CD73-positive cells expressed CD90, the latter not expressed on endothelial cells.

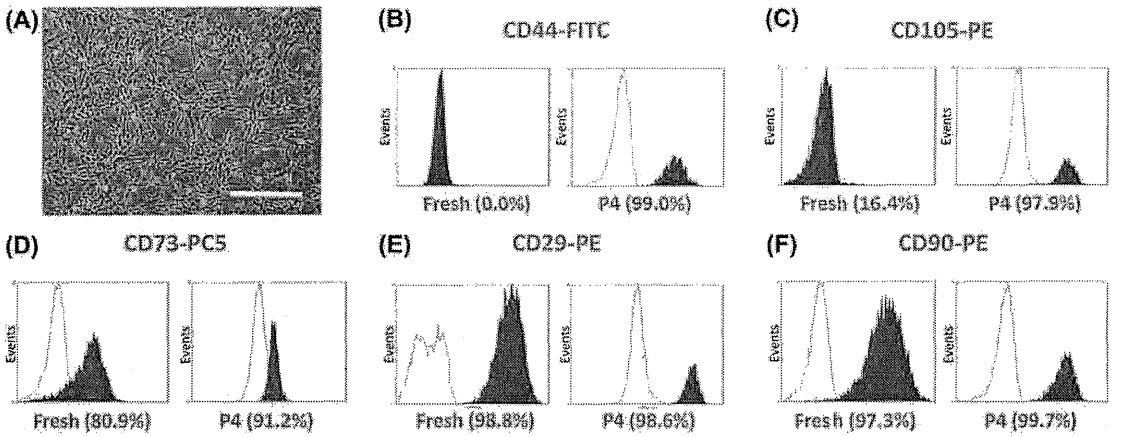

Figure 3. Changes in cell-surface markers associated with *in vitro* expansion. (A) Phase-contrast image of expanded UCMS cells. After *in vitro* expansion, analysis of MSC markers revealed an increased expression of CD44 (B), CD105 (C) and CD73 (D). In contrast, no change was observed in the expression of CD29 (E) and CD90 (F) because of *in vitro* expansion. Scale bar, 100 μm (A).

in multiple cell types including mesenchymal cells) and CD73 (Figure 3D; a nucleotidase expressed by multiple cells including mesenchymal cells) was increased in cells at passage 4. In contrast, expression of CD29 (Figure 3E; an integrin expressed in MSC) and CD90 (Figure 3F; a glycophosphatidylinositol-anchored cell-surface protein expressed by multiple cells including MSC) was similar to that observed prior to *ex vivo* expansion. These profiles were similar to amniotic-derived MSC as reported by De Coppi *et al.* (40).

Potential of UCMS cells

To investigate the potential of isolated UCMS cells to form differentiated cell types, the cell population was expanded under conditions conducive for osteocyte, chondrocyte or adipogenic differentiation. Under conditions conducive to the formation of osteocytes, on day 31 in cell culture Alizarin Red S-positive mineralized matrix-like nodules were observed (Figure 4A) and analysis of RNA confirmed the expression of osteocyte markers, osteopontin and alkaline phosphatase (ALP) (Figure 4B). Similarly, under conditions conducive to formation of a chondrogenic pellet, on day 21 in cell culture, Alcian Blue-positive chondrogenic-like pellets were observed (Figure 4C) and analysis of RNA confirmed the expression of chondrocyte markers, Sox-9 and aggrecan (Figure 4D). Under conditions leading to the formation of adipocytes, on day 20 of cell culture, Oil Red O-positive cells with lipid droplets were observed (Figure 4E, F) and analysis of RNA confirmed the expression of adipocyte marker peroxisome proliferator-activated receptor PPARγ2 (Figure 4G). Similarly, isolated cells incubated under conditions leading to neuronal differentiation showed subsequent expression of microtubule-associated protein 2 (MAP-2) and glial fibrillary acidic protein (GFAP) (Figure 4H). Furthermore, differentiated UCMS cells showed the myocyte marker MyoD (Figure 4I) and glucagon as a pancreatic cell marker (Figure 4J) when incubated under conditions leading to the formation of myocytes and pancreatic cells, respectively.

Suppression of GvHD by UCMS cells transplantation

In vitro-expanded MSC have been shown to suppress GvHD in patients after hematopoietic stem cell transplantation (41). To evaluate the potential for non-expanded UCMS cells to suppress GvHD, mice underwent allogeneic hematopoietic stem cell transplantation and were treated with non-expanded UCMS cells in RPMI. As a control, mice underwent allogeneic hematopoietic stem cell transplantation and were treated with RPMI alone. Mice were treated with non-expanded UCMS on days 0 and 6 after allogeneic stem cell transplantation, and the survival rate and severity of GvHD were investigated by 25 weeks after Bone Marrow Transplantation. (BMT). The frequency of severe GvHD at 6 weeks after allogeneic stem cell transplantation was significantly reduced with concomitant transplantation of non-expanded UCMS cells (Figure 4A). Although all mice in the control group showed severe GvHD or were already dead at 6 weeks, none of those treated with non-expanded UCMS cells (after the second treatment) were dead or showed severe GvHD. Representative pictures at 6 weeks in control and UCMS groups are shown in Figure 4B, C, respectively. Figure 4D shows the survival curve after allogeneic hematopoietic stem cell transplantation. Although no

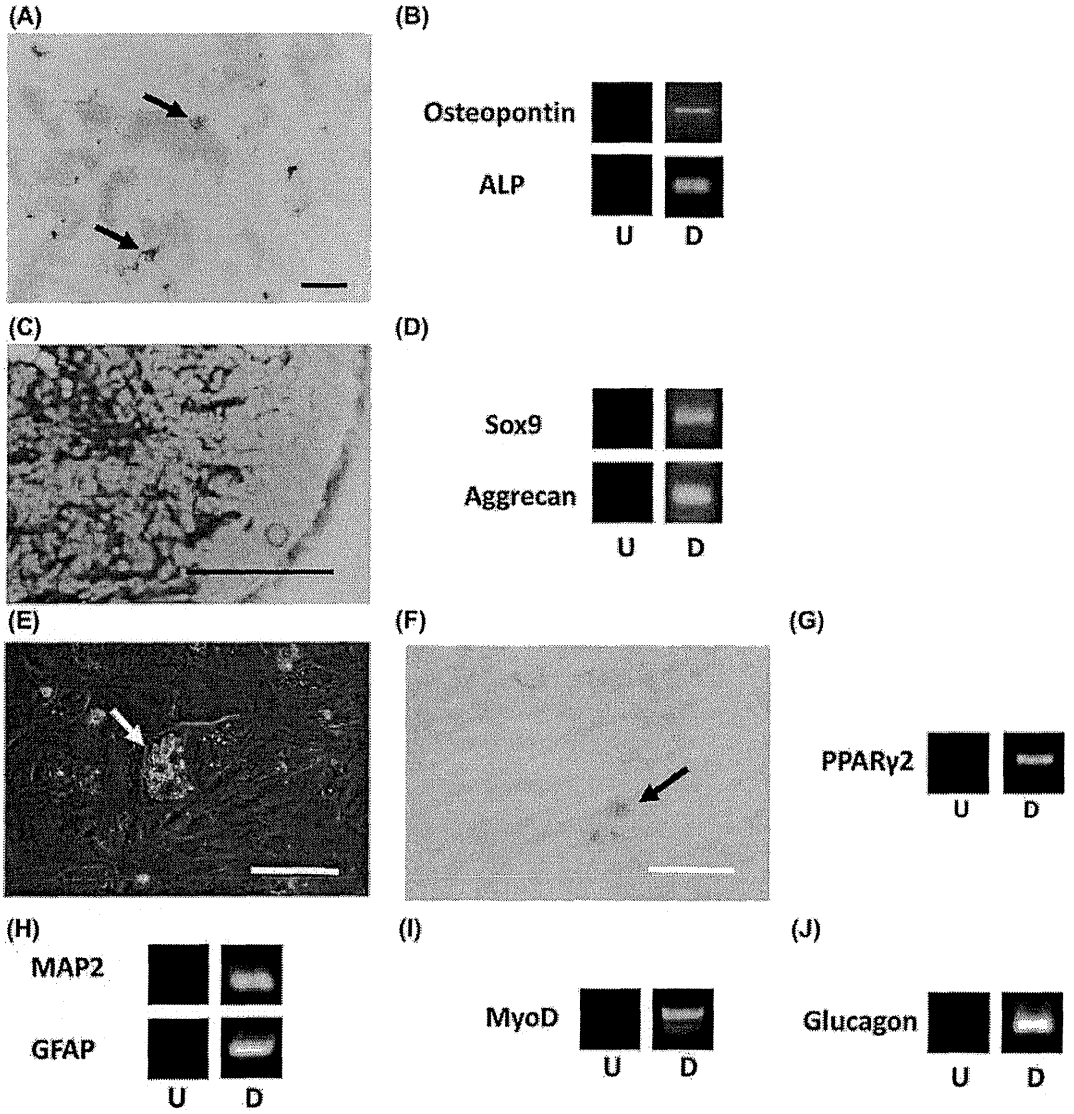

Figure 4. *In vitro* differentiation of freshly isolated UCMS cells. After expansion under conditions conducive to osteocyte or chondrocyte differentiation, Alizarin Red S-positive mineralized matrix-like nodules (A) or Alcian Blue-positive chondrogenic-like pellets (the latter displayed formation of layered structure at the surface) (C), respectively, were observed. UCMS cells cultured under conditions conductive to differentiation of osteocyte (B) and chondrocyte (D) cells expressed specific markers for each lineage. After expansion under conditions conducive to adipocyte differentiation, Oil Red O-positive adipocytes (E, phase-contrast image; F, Oil Red O staining) were observed and expression of PPARγ2 was observed (G). UCMS cells cultured under conditions conductive to differentiation of neuronal (H), myocyte (I) and pancreas (J) cells expressed specific markers for each lineage. Each experiment was repeated five times using different umbilical cord-derived cells. Scale bar, 40 μm (A), 100 μm (C, E, F). The arrow indicates Alizarin Red S-positive mineralized matrix-like nodules (A), lipid droplet (E) and Oil Red O-positive cells (F). U, undifferentiated; D, differentiated (B, D, G–J).

significant difference was apparent between groups at the 4-week assessment point, all of the mice in the control group were dead in 25 weeks, whereas no death was observed in mice with UCMS treatment group after the second treatment (Figure 5D).

Discussion

This study demonstrates that more than 2×10^7 MSC can be obtained safely from human umbilical cord without *in vitro* expansion and that these non-expanded MSC have the potential to suppress GvHD.

As a source of MSC, the umbilical cord has major advantages, including little contamination by cells of maternal origin, easy sterilization and few ethical problems. Compared with the method described by Weiss *et al.* (29), our modified method omits removal of blood vessels from the umbilical cord before treatment with collagenase and hyaluronidase.